Michigan Ion Beam Laboratory
FOR SURFACE MODIFICATION AND ANALYSIS

ANNUAL RESEARCH REPORT

2014

Gary S. Was, Director
Ovidiu Toader, Operations Manager
Fabian Naab, Engineer

2600 Draper Road
Department of Nuclear Engineering and Radiological Sciences
University of Michigan
Ann Arbor, Michigan 48109-2145
http://www.ners.engin.umich.edu/research/mibl/

Telephone: (734) 936-0166 Fax: (734) 763-4540

The Annual Research Report

This report summarizes the principal research activities in the Michigan Ion Beam Laboratory during the past calendar year. One hundred thirty researchers conducted fifty-two projects at MIBL that accounted for over 6577 hours of instrument usage. The programs included participation from researchers at the University, corporate research laboratories, private companies, government laboratories, and other universities across the United States. The extent of participation of the laboratory in these programs ranged from routine surface analysis to ion assisted film formation. Experiments included Rutherford backscattering spectrometry, elastic recoil spectroscopy, nuclear reaction analysis, direct ion implantation, ion beam mixing, ion beam assisted deposition, and radiation damage by proton bombardment. The following pages contain a synopsis of the research conducted in the Michigan Ion Beam Laboratory during the 2013 calendar year.

About the Laboratory

The Michigan Ion Beam Laboratory for Surface Modification and Analysis was completed in October of 1986. The laboratory was established for the purpose of advancing our understanding of ion-solid interactions by providing up-to-date equipment with unique and extensive facilities to support research at the cutting edge of science. Researchers from the University of Michigan as well as industry and other universities are encouraged to participate in this effort.

The lab houses a 1.7 MV tandem ion accelerator, a 400 kV ion implanter, and an ion beam assisted deposition (IBAD) system. Additional facilities include a vacuum annealing furnace, a surface profilometry system, and a scanning laser surface curvature measurement system. The control of the parameters and the operation of these systems are mostly done by computers and are interconnected through a local area network, allowing off-site monitoring and control.

In 2010, MIBL became a Partner Facility of the Advanced Test Reactor, National Scientific User Facility (ATR-NSUF), at Idaho National Laboratory, providing additional opportunities for researchers across the US to access the capabilities of the laboratory. In 2013, MIBL hosted four ATR projects.

On December 20, 2013, the lab was closed for a major expansion that includes the addition of a 3 MV tandem accelerator, reconfiguration of the accelerator room, establishment of a target room and a control room and coupling of the three accelerators to provide the capability to conduct dual and triple beam ion irradiations. All of the new capabilities will be active in 2014.

Respectfully submitted,

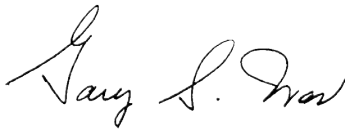

Gary S. Was, Director

RESEARCH PROJECTS

ACCELERATED IRRADIATIONS FOR EMULATION OF HIGH-DOSE MICROSTRUCTURE IN FERRITIC-MARTENSITIC STEELS

A.M. Monterrosa, Z. Jiao, G.S. Was
Department of Nuclear Engineering and Radiological Sciences, University of Michigan

The new generation of faster reactors is seeking to push damage levels in structural materials to very high doses, in excess of 200 dpa. Using fast reactors to irradiate materials to such high doses is prohibitively expensive and time-consuming. This project will study how effectively self-ion irradiations can be used to emulate microstructural features (voids and precipitates) seen in neutron-irradiated HT9 and other ferritic-martensitic (F-M) steels.

Self-ion irradiation experiments have been performed on ferritic-martensitic alloys HT9 and T91 to determine swelling behavior from 400°C-460°C and up to 188 dpa with up to 10 atomic parts per million (appm) helium pre-implanted. The irradiations were performed in the Tandetron accelerator at the Michigan Ion Beam Laboratory. The effects of dose and temperature on void swelling were analyzed using a transmission electron microscope in scanning mode (STEM). The size, density and distributions of radiation-induced voids were analyzed through the depth of the microstructure. Swelling values of 4.8% and 2.5% in HT9 and T91 respectively were observed at 460°C at a dose of 188 dpa and a depth between 500-700nm. Results were compared with those from the same heats irradiated in FFTF. Future work will include reaching even higher doses to confirm a steady-state swelling rate and an optimization of parameters to mimic the results found in neutron irradiations.

This work is supported by DOE NEUP award DE-AC07-05ID14517.

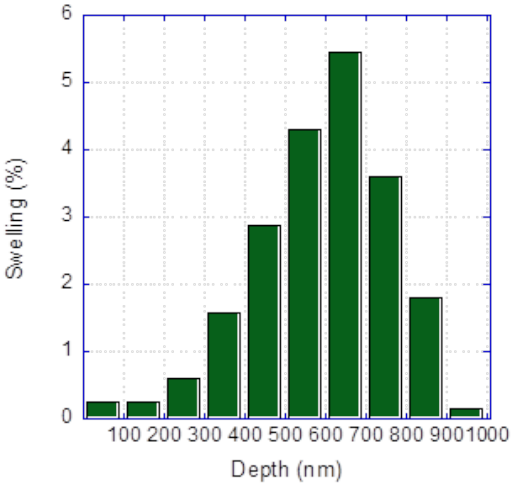

Swelling profile in HT9 at 460°C, 188 dpa.

Sample	Irrad.	T (°C)	Dose (dpa)	Void Size (nm)	Void Density (m^{-3})	Swelling (%)
HT9 FFTF	Reactor	410	100	18	7.5×10^{19}	0.02
HT9 FFTF	Reactor	440	150	28	2.5×10^{20}	0.3
T91 FFTF	Fe^{++} ion	410	184	29	8.3×10^{20}	1.6
HT9-10He	Fe^{++} ion	440	150	9.56	1.95×10^{19}	0.00061
HT9-10He	Fe^{++} ion	460	188	32.6	18.7×10^{20}	4.88
HT9-1He	Fe^{++} ion	460	188	26.87	3.7×10^{20}	0.63
T91-10He	Fe^{++} ion	460	188	25.9	19.3×10^{20}	2.51
T91-1He	Fe^{++} ion	460	188	21.7	9.5×10^{20}	0.75

Swelling comparison between neutron and heavy-ion experiments.

ANISOTROPY OF DISLOCATION LOOPS FROM IN-SITU PROTON IRRADIATION CREEP

C. Xu, G.S. Was
Department of Nuclear Engineering and Radiological Sciences, University of Michigan

In-situ irradiation experiments have been conducted to explore the anisotropy in the microstructure of irradiation creep FM steel samples. Alloy T91 was irradiated with 3.2 MeV protons at temperatures between 400 and 550°C and under stresses between 100 and 200 MPa to a dose of about 1 dpa. Focused Ion Beam (FIB) lift-out samples were made from the irradiation creep sample for microstructure analysis with TEM and STEM. Anisotropy in the dislocation loop density is observed in the four samples subjected to in-situ proton irradiation.

TEM analysis of the irradiation creep microstructure in the <100> zone axis found large a_o<100> dislocation loops distributed homogenously within the material. Two sets of edge-on dislocation loops within a single grain were counted; and their normalized fractions were plotted against their orientation to the tensile axis. Four samples in total were analyzed and the ratios of the loop size and loop density are plotted in the as a function of stress and temperature in the figure. The anisotropy in the dislocation loop density was found to increase as a function of applied tensile stress, providing microstructural evidence for the operation of SIPN irradiation creep mechanism in FM steels.

Support for this research was provided by the Department of Energy under NEUP grant DE-AC07-05ID14517

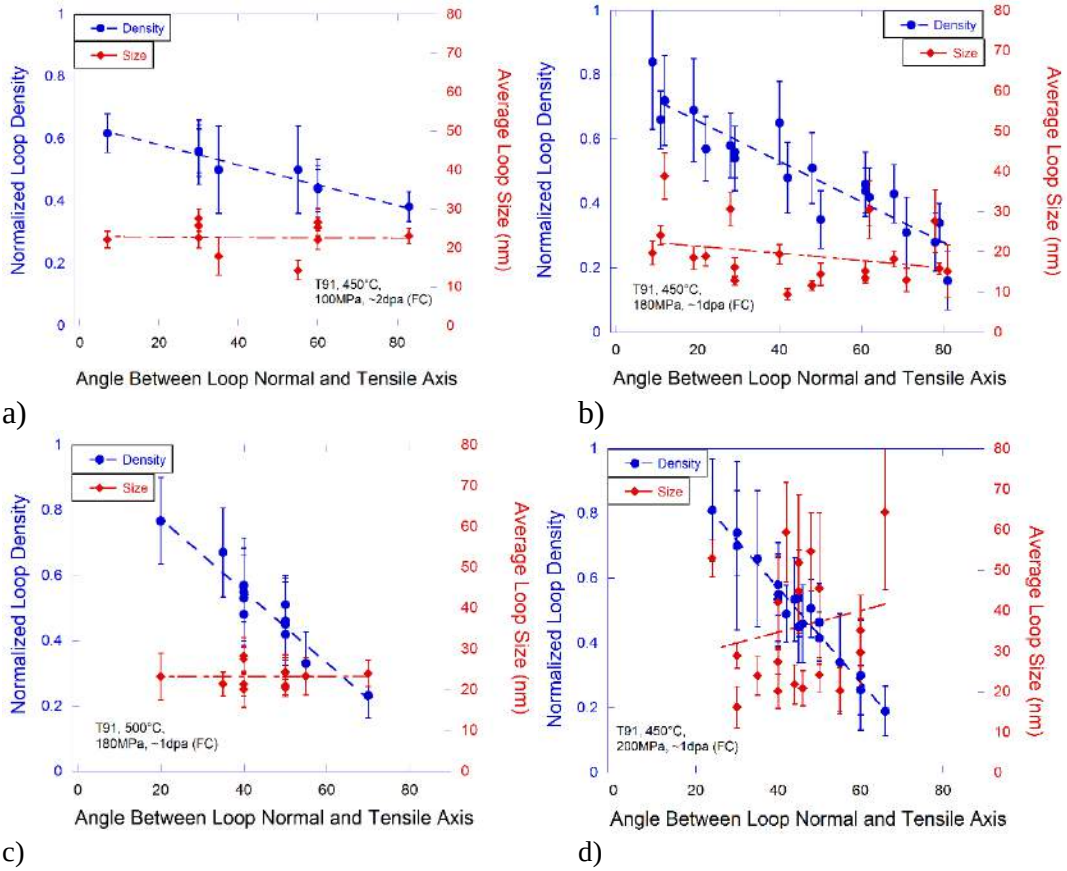

Loop anisotropy plot of the irradiation creep experiments for a) 450°C 100MPa, b) 450°C 180MPa, c) 500°C 180MPa, d) 450°C 200MPa.

POST-IRRADIATION ANNEALING AS A MITIGATION STRATEGY FOR IASCC

Z. Jiao[1], J. Hesterberg[1], G.S. Was[1], P. Chou[2]
[1]Department of Nuclear Engineering and Radiological Sciences, University of Michigan
[2]Electric Power Research Institute

Irradiation assisted stress corrosion cracking (IASCC) is the primary form of core component cracking in boiling water reactors. It is also an issue of growing importance in pressurized water reactors. The ultimate goal is not only to understand the mechanism of IASCC but to provide mitigation strategies for components under service and guide for alloy design for future reactors. Post-irradiation annealing (PIA) has been demonstrated as a potential mitigation method for IASCC in stainless steels in a few studies. However, the reason that PIA may lead to the mitigation of IASCC is not well understood. This project is intended to understand the mitigation mechanism of PIA through its relationship with localized deformation in proton-irradiated austenitic stainless steels.

Commercial grade 304SS that is very susceptible to IASCC in simulated BWR environment was selected for this study. Samples were irradiated to 10 dpa using 2 MeV protons at 360°C at Michigan Ion Beam Laboratory (MIBL). Cracking susceptibility was mitigated after PIA at 500°C:1h and fully eliminated after PIA at 600°C:10h. Additional heat treatments are being studied in an effort to pinpoint the conditions at which IASCC susceptibility is eliminated.

Support for this research was provided by the Electric Power Research Institute (EPRI)

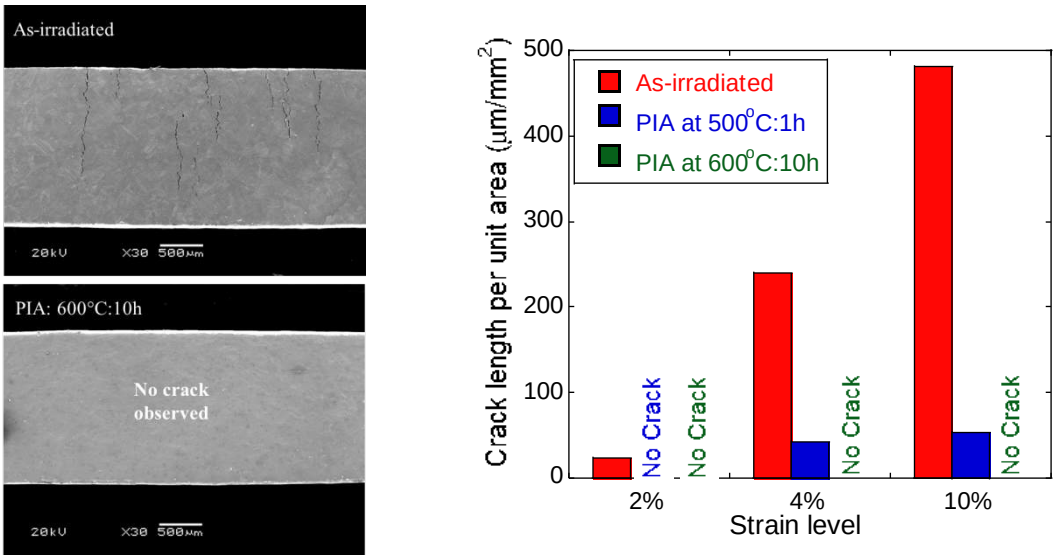

Comparison of cracking susceptibility of CP304, as-irradiated (360°C:10dpa) and after PIA at different conditions, in simulated BWR NWC environment. The right images are after 10% strain.

ESTABLISHING A CAUSE-AND-EFFECT RELATIONSHIP BETWEEN LOCALIZED DEFORMATION AND IASCC

Z. Jiao[1], J. Hesterberg[1], G.S. Was[1], P. Chou[2]
[1]Department of Nuclear Engineering and Radiological Sciences, University of Michigan
[2]Electric Power Research Institute

Irradiation assisted stress corrosion cracking (IASCC) is the primary form of core component cracking in boiling water reactors. It is also an issue of growing importance in pressurized water reactors. This project aims to establish direct evidence of a cause-and-effect relationship between localized deformation and IASCC, aided by improved methods for quantifying crack initiation, and to develop an understanding of how localized deformation leads to IASCC. The leading IGSCC mechanism is slip-oxidation, in which rupture of the oxide film above the grain boundary leads to exposure of the underlying alloy to the solution, causing rapid oxidation. The direct role of dislocation channels in oxide rupture at the grain boundaries thus leading to crack initiation need to be demonstrated.

Commercial grade 304SS was irradiated to 5 dpa using 2 MeV protons at 360°C at Michigan Ion Beam Laboratory (MIBL). The sample was exposed in high temperature water (320°C, 5ppm DO) for 150 hours to form 100nm thick oxides film. Cracking susceptibility was examined after straining to 2 and 4% in simulated BWR environment. No crack was observed at 2% and cracks appeared after 4% strain. Compared to the same irradiated alloy without oxides film (shown in the figure below), it appears that the 100nm-thick oxide film suppresses cracking at low strain but does not eliminate cracking at higher strain. As channel height increase with strain, the degree of localized deformation is higher at 4% compared to that at 2%. Therefore, larger channels are needed to break the oxide film for crack imitation in the sample with oxide film. It is postulated that cracking may not happen in samples with much thicker oxide film.

Support for this research was provided by the Electric Power Research Institute (EPRI)

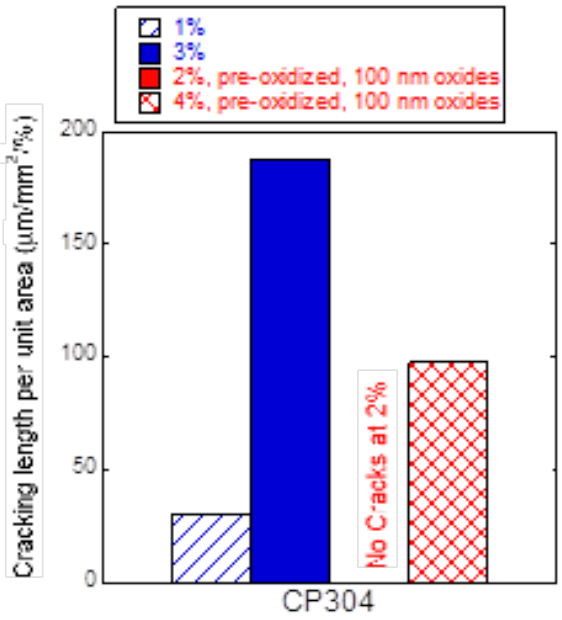

Comparison of cracking susceptibility of irradiated CP304 (360°C:5dpa) with (red) and without (blue) 100nm thick oxide film in simulated BWR NWC environment.

PHASE STABILITY IN SELF-ION IRRADIATED FERRITIC-MARTENSITIC ALLOYS AT HIGH FLUENCES

Z. Jiao, A. Monterrosa, E. Beckett, K. Sun, G.S. Was
Department of Nuclear Engineering and Radiological Sciences, University of Michigan

Understanding microstructure development in materials irradiated to high dose is, in a sense, the holy grail of materials performance in reactor systems. Fast reactor ducts will likely see damage levels of 200 dpa, and for the Traveling Wave Reactor to become a reality, the clad and some structural materials must withstand 500-600 dpa. This high dose level is unrealistic for test reactors to achieve in a reasonable time frame. As such, only ion irradiation is capable of providing the required levels of damage in reasonable time frames. F-M alloys may be subject to radiation-induced embrittlement due to the precipitation of new phases under irradiation. Data on precipitation at high doses are especially lacking due to the great limitation of test reactors. The objective is to understand the evolution of radiation-induced precipitates in F-M alloys following self-ion irradiation to high doses.

Ferritic-martensitic alloys (T91, HCM12A and HT9) were irradiated up to 250 dpa (SRIM in KP mode) at temperatures 400-500°C at MIBL. Radiation-induced precipitates were investigated using atom probe tomography (APT). Typically, four types of precipitates were observed in heavy-ion irradiated F-M alloys. They are Ni/Si-rich, Cu-rich and Cr-rich precipitates and Cr-rich carbides. Irradiation to high dose or at high temperature causes coarsening of the precipitates. Formation of Cr_6C is observed in HCM12A following irradiation to 500°C:250dpa as shown in the figure below.

Support for this research was provided by the U.S. DOE under contract DE-FG07-07ID14894, and DE-AC07-05ID14517.

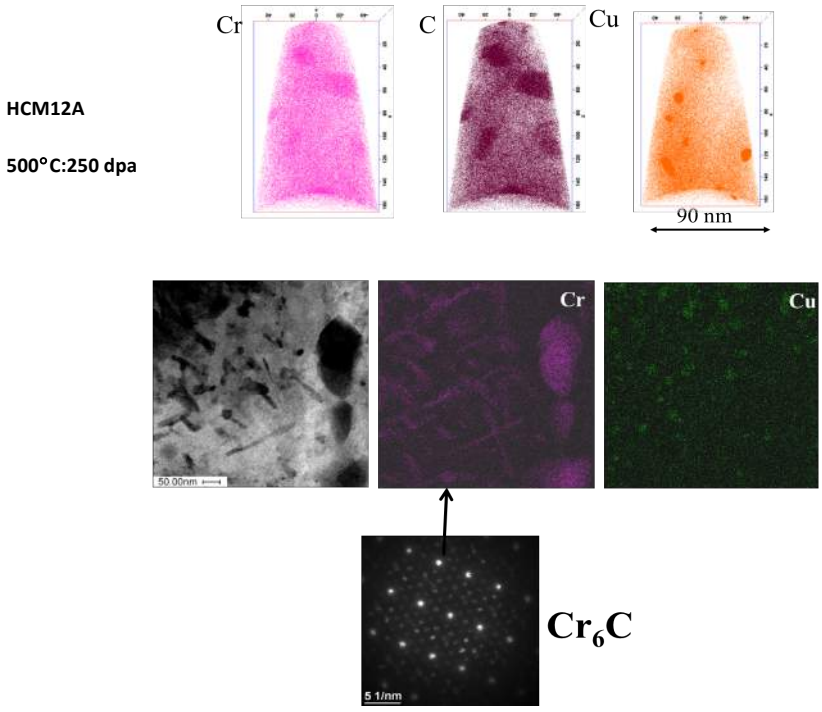

Formation of Cr_6C carbides in HCM12A following Fe^{++} irradiation to 250 dpa at 500°C as shown by APT (top images), TEM-EDS and the diffraction pattern.

IRRADIATION EFFECTS IN FERRITIC-MARTENSITIC STEELS AT VERY HIGH DOSES

E.M. Beckett, Z. Jiao, K. Sun, G.S. Was
Department of Nuclear Engineering and Radiological Sciences, University of Michigan

This project will study the effects of very high doses of heavy ion irradiation, up to 400 dpa (KP calculation), in HT9 and other ferritic-martensitic (F-M) steels, in the range of 400-500°C, which is the anticipated operating temperature regime of the TerraPower, LLC traveling wave reactor. Of greatest interest is the microstructural evolution under irradiation, including void swelling, dislocation loop nucleation and growth, and precipitation.

Self-ion irradiation experiments have been performed on ferritic-martensitic alloy HT9 to determine swelling behavior at 440°C to doses of 280 dpa and above using three concentrations of pre-implanted helium. Irradiations were performed on both helium pre-implanted and unimplanted samples using raster scanning on a Tandetron accelerator at the Michigan Ion Beam Lab. The effects of helium pre-implantation on bulk swelling were determined by examining the void distribution using transmission electron microscopy (TEM) and in samples implanted with 0, 10 and 100 atom parts per million (appm) helium. Additionally, atom probe tomography (APT) was used to examine the effect of helium on precipitate formation. Helium implantation was not required to for void formation at doses of 140 dpa and above. The addition of helium increased average size, void density and void swelling. Void density was most affect by the addition of helium as helium greatly enhances void nucleation, but the effect of growth is less clear.

Future work will include reaching even higher doses to more fully map out the swelling curve at different temperatures.

This work is supported by TerraPower, LLC.

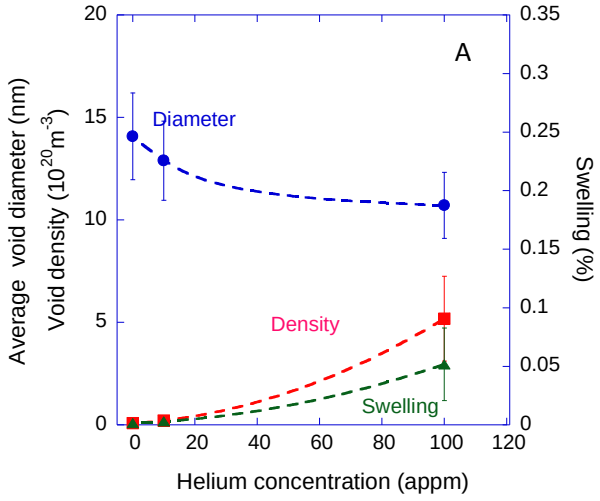

Diameter, number density and swelling at 440°C, 140 dpa.

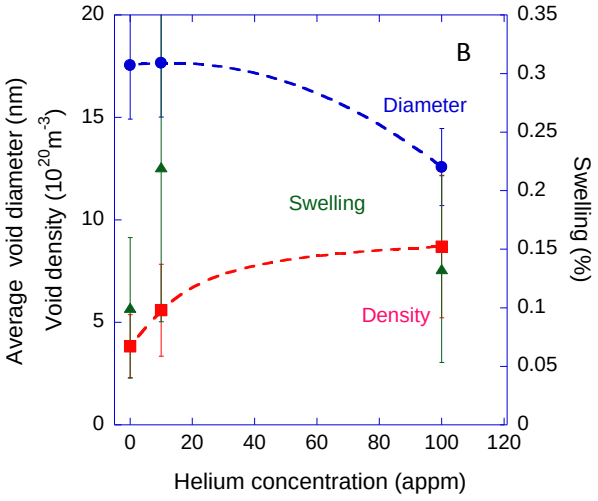

Diameter, number density and swelling at 440°C, 188 dpa.

STRONTIUM DIFFUSION IN SILICON CARBIDE

S. Dwaraknath, G.S. Was
Department of Nuclear Engineering and Radiological Sciences, University of Michigan

This project focused on identifying the mechanism for strontium diffusion into silicon carbide (SiC) in support of TRISO fuel licensing and the very high temperature reactor (VHTR) program. High temperature multi-layered diffusion couples were fabricated and consisted of a SiC substrate, a thin layer of pyrolytic carbon (PyC), followed by a final coating of SiC. The PyC was ion implanted with strontium to a fluence of 10^{16} cm^{-2} at the Michigan ion beam laboratory (MIBL) using the 400 keV ion implanter. The implanted fluence was verified by Rutherford backscattering spectroscopy (RBS) performed at MIBL. The diffusion couple was annealed at 1100ºC for 10 hours. RBS was used to verify the integrity of the diffusion couple post-annealing. The figure shows a secondary ion mass spectrometry (SIMS) depth profile of a diffusion couple after annealing. The SIMS profile shows strontium diffusing approximately 520 nm into the SiC.

This work is supported by the Department of Energy under NEUP Contract #00103195

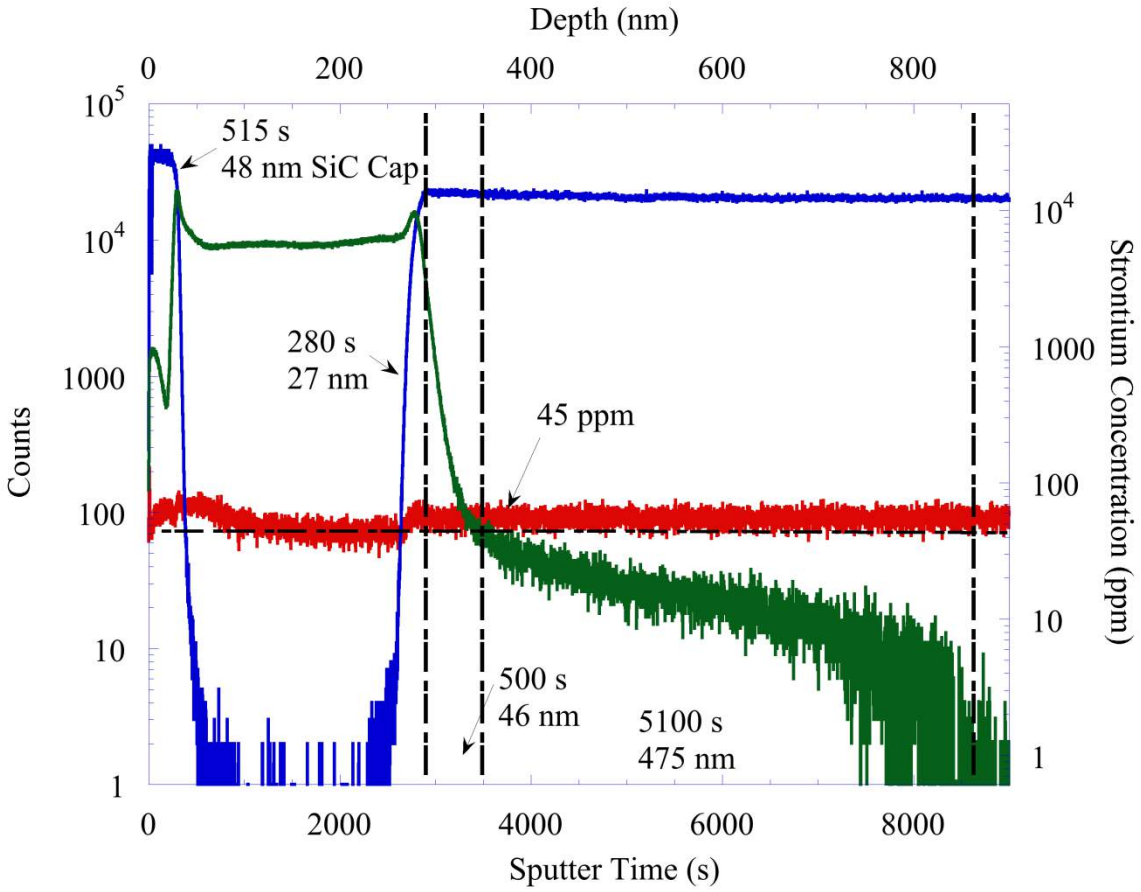

Secondary ion mass spectrometry (SIMS) depth profile of a strontium diffusion couple showing strontium diffusion approximately 520 nm into the SiC substrate following annealing at 1100ºC for 10 hours.

IN-SITU STUDY OF IRRADIATION ACCELERATED CORROSION OF ZIRCALOY-4 IN PWR ENVIRONMENT

P. Wang, G.S. Was
Department of Nuclear Engineering and Radiological Sciences, University of Michigan

This project aims to understand how radiation accelerates corrosion of Zircaloy-4 fuel cladding. Limited data indicates that the radiation effect is large; it causes order of magnitude increases in corrosion rates. This work will address the process of irradiation-accelerated corrosion (IAC) and improve understanding of the role of irradiation in the corrosion process.

A 50 μm thin zircaloy-4 sample has been hydraulically formed and then laser welded to the sample mount (zirconium alloy) shown in Fig 1. A miniature corrosion cell was built to fit on the end of the beamline, serving as an autoclave with water circulation system attached. The thin sample served as a window to separate ultra-high vacuum in the beamline and over 1800 psi water pressure in the corrosion cell, and still allow 3.2 MeV proton beam to fully pass through, while maintaining water pressure at 320°C. A dedicated beamline was constructed and fast valves were installed in case of sample rupture.

Over the last year, zirconium samples were fabricated and tested to fulfill the requirements for the irradiation experiment, e.g. leakage free, burst pressure test, electrical isolation, etc. A Zircaloy-4 sheet (initial thickness of 450 μm) was precision lapped and polished down to 50 μm, and laser welded onto a pre-oxidized zirconium alloy mount that was designed for the corrosion cell. To measure the corrosion potential during irradiation, the cell was electrically isolated using a pre-oxidized zirconium seal, and insulation from the beamline was done using a ceramic break. A Pd/Pt reference electrode was used to measure electrochemical corrosion potential between the zirconium samples using a Gamry Ref 600 potentiostat.

Several experiments were performed using the setup described above, and the results are promising, accelerated corrosion behavior has been observed, up to 5x thicker oxide had formed on the in-situ irradiated sample (dose rate at 1.6×10^{-6} dpa/s for 24 hr). Figure 2 shows the difference between the irradiated and unirradiated sample oxide thicknesses.

This work is supported by the U.S. Department of Energy under grant DE-AC07-05ID14517, and closely collaborated with Dr. David Bartels at University of Notre Dame.

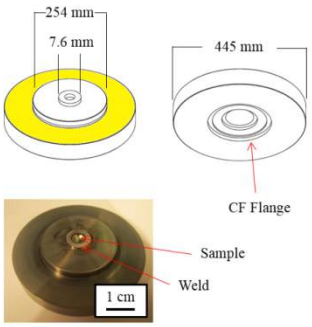

Figure 1. Sample and sample mount construction for IAC experiments.

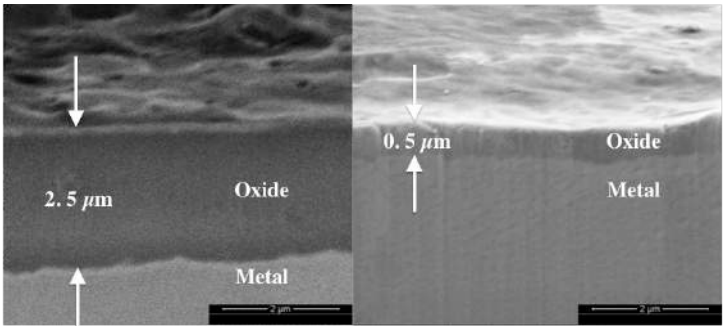

Figure 2. Oxide thickness of the irradiated (left) and unirradiated (right) portions of a Zr-4 sample after 24 hr in pure water containing 3 ppm H at 320°C.

IRRADIATION ACCELERATED CORROSION OF REACTOR CORE MATERIALS

S.S. Raiman, P. Wang, G.S. Was
Department of Nuclear Engineering and Radiological Sciences, University of Michigan

Corrosion of stainless steel components in nuclear reactor pressure vessels has long been a concern for the nuclear power industry. In addition to the chemically aggressive environment and high temperature, radiation has been shown to greatly accelerate corrosion in stainless steel. A fundamental understanding of the mechanisms behind irradiation accelerated corrosion (IAC) is needed for both the life-extension of LWRs, and for use in designing materials for Gen IV concepts.

A specially designed facility was constructed at the Michigan Ion Beam Laboratory to study irradiation accelerated corrosion. To allow for simultaneous irradiation and oxidation, a proton beam passes through a very thin sample, which serves as a "window" into a corrosion cell filled with flowing high pressure, high temperature water. By allowing the proton beam to pass completely through the sample, the effects of radiation in both the solid and in the solution can be studied simultaneously.

Experiments were conducted on samples made from Type 316L stainless steel sheet stock formed to 37 μm thick at the center. Samples were exposed to 320˚C water with 3 ppm H_2 for 24 hours.

This research is supported by the DOE NEUP, grant number DE-AC07-05ID14517, and EDF contract no. 8610-BVW-4300243004.

7 x 10^{-6} dpa/s
• Inhomogeneous morphology
• Appears to be composed of precipitates

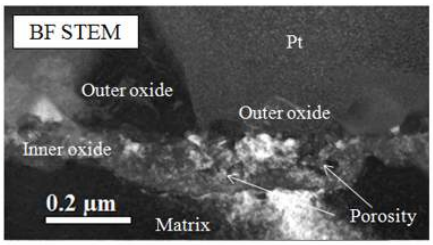

Radiolyzed water only
• More homogeneous morphology
• Consistent with inward growth

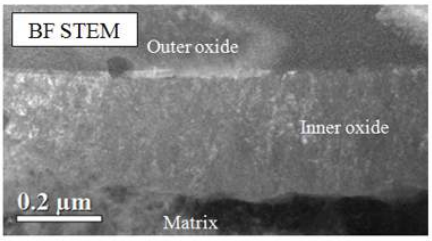

Unirradiated
• More homogeneous morphology
• Consistent with inward growth

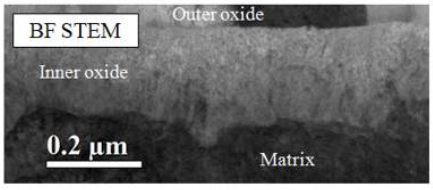

Cross-sectional STEM images of oxides from three surfaces, an irradiated surface (top), an unirradiated surface exposed to radiolyzed water (center) and an unirradiated surface (bottom). The irradiated inner oxide appears porous an inhomogeneous compared to the oxides not exposed to direct radiation.

ACCELERATED STRESS CORROSION CRACK INITIATION OF ALLOYS 690 AND 600

T. Moss, G.S. Was
Department of Nuclear Engineering and Radiological Sciences, University of Michigan

In this project, stress corrosion crack (SCC) initiation susceptibility of alloys 690 and 600 is studied. At normal operating temperatures, little to no cracking is observed in alloy 690. To study the SCC behavior, the cracking must be accelerated which can be achieved by increasing the test temperature. However, the normal testing temperature of 360°C is already very close to the supercritical point (374°C), so accelerated tests will need to be conducted in the supercritical regime. There is some question as to whether the cracking mechanism in supercritical water is the same as in subcritical water. In order to determine if there is a mechanism change, tensile samples of alloys 690 and 600 are strained in a constant extension rate tensile (CERT) test and the amount of cracking is measured between 320°C and 450°C at a constant distance away from the Ni/NiO boundary. The amount of cracking is used to calculate the activation energy for crack initiation.

A change in the oxidation behavior (structure, morphology, or chemistry) could also be an indication that there may be a different cracking mechanism. Coupons of alloy 690 and alloy 600 were exposed at 400°C and 360°C to evaluate the oxidation behavior in subcritical and supercritical water. To determine the oxide thickness of the coupons, nuclear reaction analysis (NRA) was performed using an 850 keV D^+ beam to measure the protons from the $^{16}O(d,p_1)^{17}O$ reaction as shown in the figure on the left. To determine how much of an oxide formed, a ratio was taken between the number of counts in the $^{16}O(d,p_1)^{17}O$ peak and the integrated charge for each condition as shown in the figure on the right. The NRA analysis was vital in determining quantitatively the oxide evolution with time.

This research is supported by EPRI Contract #EP-P35621.

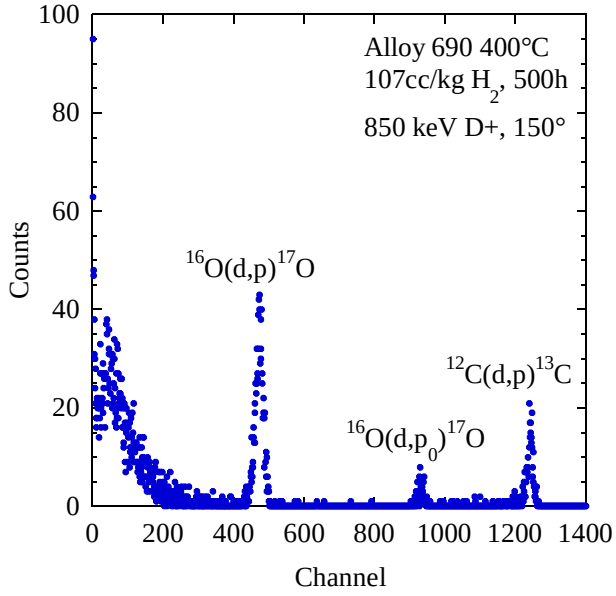

Example of NRA data taken from alloy 690 exposed at 400°C with 107cc/kg dissolved hydrogen for 500h.

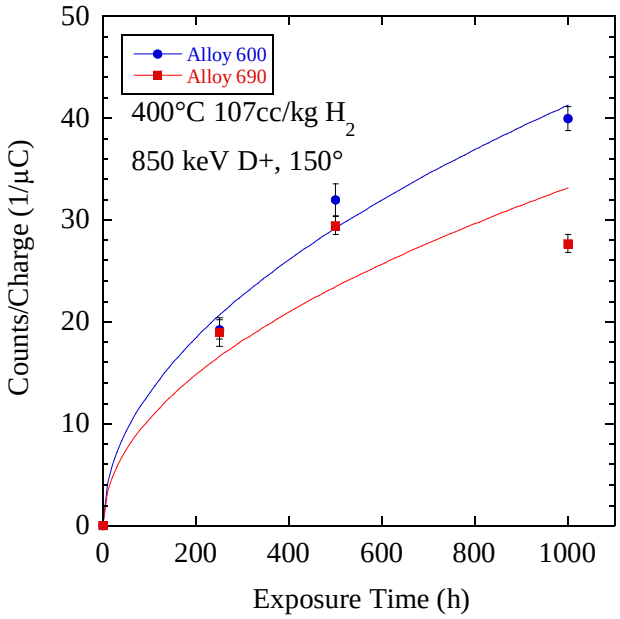

Oxygen content on the surface of Alloy 600 and Alloy 690 coupons as a function of exposure time.

EVALUATION OF MATERIALS FOR INTERIM STORAGE OF USED FUEL FOR MORE THAN 100 YEARS

F. Zhang, L.M. Wang
Department of Nuclear Engineering & Radiological Sciences, University of Michigan

Al/B_4C metal matrix composite (MMC) is an important neutron absorbing material used in both wet storage pools and dry storage casks of spent nuclear fuel for preventing criticality. Because of the high neutron absorption cross-section of ^{10}B, the material can effectively absorb fast and thermal neutrons, but at the same time suffers irradiation damage from the nuclear spent fuel. Moreover, interactions of fast and thermal neutrons with boron lead to the production of several transmutation species such as helium, lithium and others, according to the transmutations reactions induced by neutron irradiation, including the ^{10}B (n, ^{4}He) ^{7}Li reaction and others. The most abundant product of these reactions is energetic helium (~1.47MeV), which may induce further radiation damage and be precipitated out in the material as helium bubbles. The formation and distribution of the helium bubbles may affect the mechanical and chemical performance of the material in its working environment. In this experiment, the combined ion irradiation, which is helium implantation and proton irradiation, was performed to simulate the bubble formation, neutron interactions with boron and neutron irradiation damage.

The bulk sample was pre-implanted with 400keV He^+ to 1.0×10^{16} ions/cm^2 at room temperature and then irradiated with 1.5MeV proton to 2.2×10^{19} ions/cm^2 at 110℃ in Michigan Ion Beam Laboratory (MIBL). The depth for macrostructure analysis was marked as green rectangle in Figure (d).

This work has been supported by the US DOE NEUP Program under the contract No. DE-AC07-05ID14517.

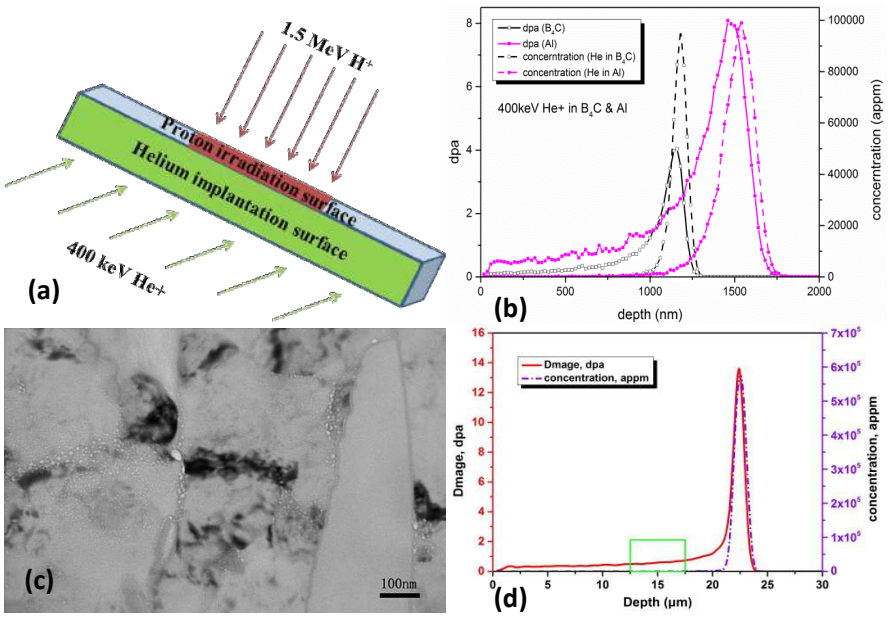

(a) is the diagram of He^+ pre-implantation and proton irradiation; (b) and (d) are SRIM results of damage production and incident gas concentration profiles in Al and B4C irradiated by 400keV He^+ and 1.5MeV proton; (c) BF image from an area in the peak He ion range with relatively larger He bubbles clearly visible in Al matrix and on grain and phase boundaries.

NANOPOROUS SEMICONDUCTORS PROCESSED BY ION BEAM IRRADIATION WITH POTENTIAL APPLICATION IN HYDROGEN STORAGE*

G. Sang[1,2], F. Zhang[2], G. Yu[2], L.M. Wang[2]
[1] Department of Chemical Engineering, University of Michigan
[2] Department of Nuclear Engineering and Radiological Sciences, University of Michigan

Ion beam irradiation has induced a unique sponge-like nanoporous structure in a group of semiconductor materials, including Ge, GaSb and InSb. Cross-sectional electron microscopy observation has revealed the progressive formation process of such a structure under ions of various mass and energy with increasing ion fluence. A radiation induced void nucleation and growth mechanism instead of surface sputtering is found to be responsible for the formation of such a structure. The morphology of the structure is stabilized at a certain ion fluence for each material with the final pore size in the range of 50-100 nm and nanofibers of about 10 nm in diameter separating the interconnecting pores. The thickness of the nanoporous layer varies with the ion mass, energy, fluence as well as the incident angle of the ions. Because of the enormous surface area and number of possible dangling bounds at the fiber surface, it is believed that such a porous structure may have a great potential for hydrogen storage. The hydrogen storage capacity of the structure will be characterized by the standard pressure–composition–temperature (PCT) method. For the PCT measurement, a large area and depth of the porous structure without a surface cover is desirable.

The three candidate materials have been irradiated at the Michigan Ion Beam Laboratory (MIBL) with Xe^+ ions in the energy range from 50 to 400 keV to explore the best irradiation condition for the measurement of hydrogen storage capacity with PCT. An example of nanoporous structures created by the Xe^+ ion irradiation is shown in the Figure. Complete characterization of all samples irradiated is still underway.

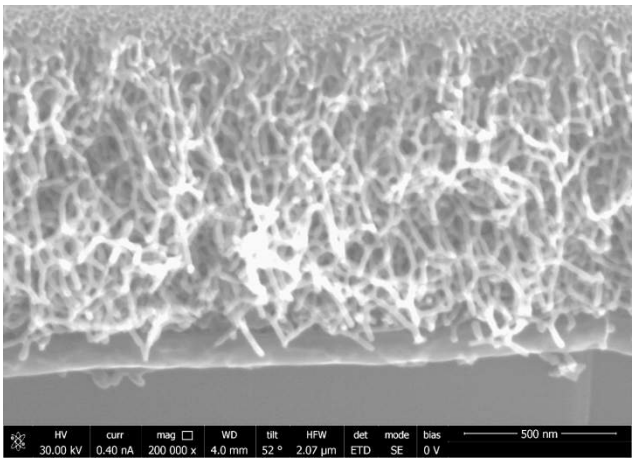

A cross-sectional SEM image showing the formation of a nanoporous structure with nanofibers of uniform thickness in GaSb after irradiating with 400 keV plus 50 keV Xe^+ ions to $2x10^{16}$ ions/cm^2 at the room temperature. The structure stretched to nearly one micrometer below the original sample surface. However, well developed nanofiber/nanopore structure is not completely exposed to the front surface of the sample (top of the image) therefore preventing the ideal measurement of hydrogen storage capacity with PCT.

*This is an exploratory research aiming at obtaining preliminary data for a new proposal on ion beam processing of hydrogen storage materials.

HIGH DOSE ION BEAM IRRADIATION OF CNS-I AND CNS-II STEELS

X. Wang, L.M. Wang
Department of Nuclear Engineering and Radiological Sciences, University of Michigan

Nuclear fusion can be one of the most attractive sources of energy from the viewpoint of safety and minimal environmental impact. Materials constitute a key issue on the path to the realization of fusion power reactors. Reduced activation materials are among the top choices for structural applications in fusion systems because of the simpler waste management and disposal. CNS (China Nuclear Steel)-I and CNS-II, two kinds of Reduced Activation Ferritic Martensitic (RAFM) steel, are produced by Institute of Nuclear Materials, University of Science and Technology Beijing (USTB). Since FM steels are potential structure materials for both advanced fast and fusion reactors, they are expected to experience high dose neutron fluence. Heavy ion irradiation will generate several orders of magnitude damage higher than neutron. We choose self-ion (Fe^{++}) irradiation to simulate the neutron radiation damage as an accelerated irradiation test.

The bulk CNS-I and CNS-II samples was pre-implanted with a series of energy helium implantations at room temperature and then irradiated with 5MeV Fe^{++} in a Tandem ion accelerator in the Michigan Ion Beam Laboratory (MIBL) at the University of Michigan. The irradiations were conducted at 460℃, and the doses of the irradiations were up to 188dpa (K-P model), Fig. (a). Both CNS-I and CNS-II showed excellent swelling resistance at 460℃ to 188dpa. Figure (b) shows the swelling comparison between CNS-I and CNS-II. The swelling volume increases from the left to the right. Overall, the CNS-II shows the less amount of swelling compared to the CNS-I, regardless of helium content.

This work has been supported by China General Nuclear Power Group.

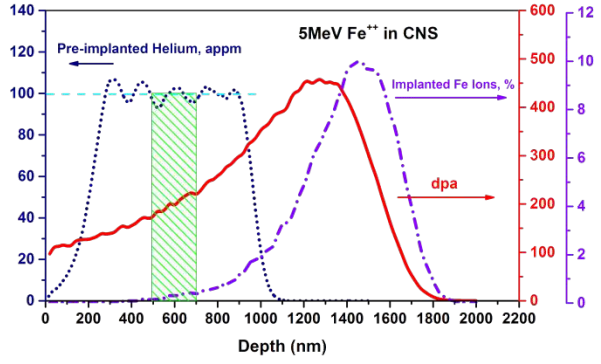

(a)

SRIM calculations for the implanted iron, helium, and damage calculations. The doses were calculated using the Kinchen-Pease model in SRIM at a depth of 600nm.

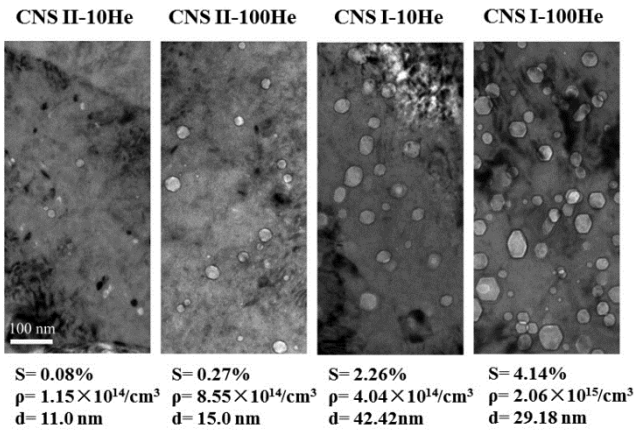

(b)

Swelling comparison in CNS.

HELIUM ION IMPLANTATION EFFECTS OF 9CR-ODS(OXIDE DISPERSION STRENGTHENED) STEEL

C.Y. Lu[1,2], Z. Lu[2], L.M. Wang[1]
[1]Department of Nuclear Engineering & Radiological Sciences, University of Michigan
[2]Key Laboratory for Anisotropy and Texture of Materials, Northeastern University, China

The oxide dispersion strengthened (ODS) reduced activation ferritic/martensitic (RAFM) steels are among the most popular candidate materials for the future fusion reactor. One important performance properties of ODS steel is its capability to absorb helium. High concentration helium will be dispersed in the structural materials in the fusion reactor. The high density nanoclusters, dislocations, grain boundaries are helpful to decrease the size of helium bubbles, minimize volume swelling and avoid helium embrittlement. In this study, 400 keV helium ions were implanted in to a 9Cr-ODS steel to study the helium bubble distribution in the steel.

The nominal composition of the 9Cr-ODS steel is Fe-9Cr-1.5W-0.4Mn-0.1Ta-0.2V-0.3Ti-0.3Y_2O_3 (wt.%). He^+ ion implantation was carried out using the 400kV NEC ion implanter at MIBL. The samples were implanted at 673K to an ion fluence of 4×10^{17} He^+/cm^2. In order to observe the depth distribution of implanted He in cross-section, focused ion beam (FIB) lift-out method was adopted for the preparation of TEM specimen by using a FEI Nova Nanolab Dualbeam. STEM analysis was conducted using a 200kV JEOL 2100F spherical aberration (Cs)-corrected Analytical Electron Microscope, including high angle annual dark field(HAADF) and bright field-STEM imaging techniques.

The depth distribution of helium bubbles in the implanted sample is shown in the figure. The helium bubbles are shown as white dots in the BF-STEM image, Figure(a), and as black dots in HAADF image because of the lower mass, Figure(b). The computer simulated damage and He concentration profiles are overlaid on the HAADF image, showing a perfect matching with the experiment results. The maximum bubble diameter in the peak He concentration region (19dpa, 20 at.% helium) is only 8.3nm±2nm.

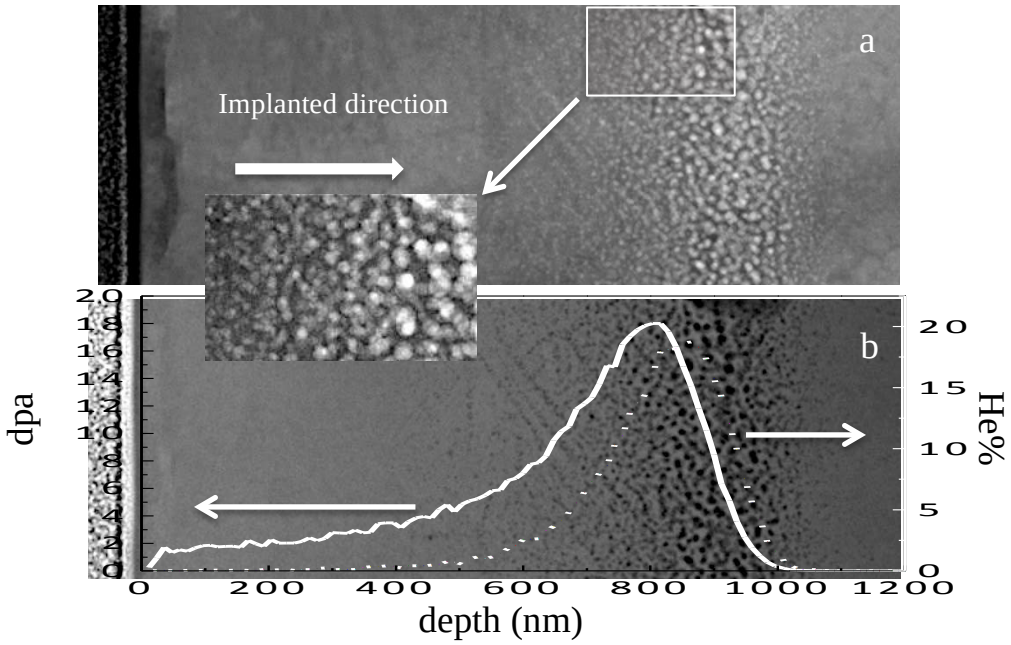

Depth distribution of helium bubble in a 9Cr-ODS steel implanted with 400keV He^+ ions at 673K to 4×10^{17} He^+/cm^2.(a) STEM-Bright Field image. (b) HAADF image overlaid with predicted damage and He concentration profiles calculated by the SRIM code.

ON THE STUDY OF THE BEHAVIOR OF A CHINA-MADE Zr-Sn-Nb ALLOY UNDER PROTON IRRADIATIONS

H.H. Shen[1,2], K. Sun[1] and X.T. Zu[2]
[1]Department of Materials Science and Engineering, University of Michigan
[2]School of Physical Electronics, University of Electronic Science and Technology of China

Zirconium and its alloys have been chosen as the fuel cladding, pressurize pipe and structure materials in the nuclear reactor primarily for their very low thermal neutron absorption cross section, good mechanical property and corrosion resistance. Although the properties of zirconium alloys have been extensively studied since 1940s, investigation on developing new type of zirconium alloy is still undergoing and in urgent, as the average fuel discharge burn-up in the reactors has steadily increased with time. This project focuses on the study of the behavior of a China-made Zr-Sn-Nb alloy under proton irradiation.

Proton irradiation was conducted at the Michigan Ion Beam Laboratory at the University of Michigan. Irradiation was conducted using 2 MeV protons to a total flux of 0.536×10^{20} H^+/cm^2, which induced a maximal damage of 45.5 dpa at the depth of 29.2 μm from the sample surface. TEM samples of the Zr-Sn-Nb alloy used in this investigation were prepared by an advanced FIB lift-out method working in a Helios 650 Nanolab workstation. Especially, the plan-view TEM specimens with different dpa value (3.9, 5.2, 7.0 and 8.2 dpa) were lifted out from the designed depth underneath the Zircaloy irradiation surface.

Results indicate that the major precipitate in the Zr-Sn-Nb-Fe-Cr alloy is $Zr(Fe,Cr,Nb)_2$ with a hcp structure same to that in the $Zr(Fe,Cr)_2$. Under 2 MeV proton irradiation at 360 ^oC, the $Zr(Fe,Cr,Nb)_2$ precipitate starts to be partially amorphized when the Zircaloy is irradiated to 3.9 dpa, and to be completely amorphized at 8.2 dpa.

This work is supported by the Fundamental Research Funds for the Central Universities of Ministry of Education of China under grant ZYGX2012YB017.

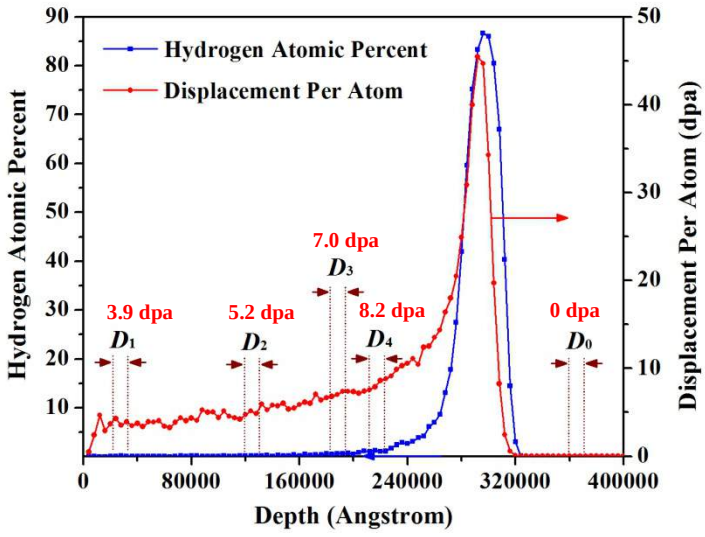

The profiles, dpa and hydrogen concentration versus depth range, calculated by SRIM program for 2 MeV proton incident on the Zr-alloy to a dose of 0.536×10^{20} H^+/cm^2 (left).

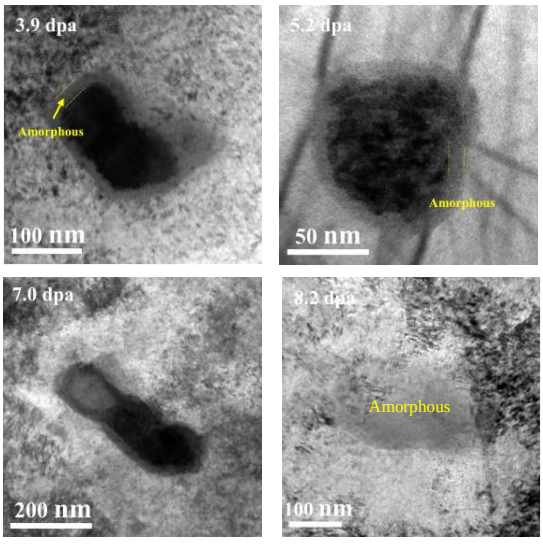

Bright-field TEM images taken from the precipitates in the Zr-alloy after having been irradiated by proton to 3.9, 5.2, 7.0 and 8.2 dpa (right), respectively.

DEVELOPMENT OF A POSITION SENSITIVE DEUTERATED LIQUID SCINTILLATOR DETECTOR

M. Febbraro, N. Anderson, F.D. Becchetti, R.O. Torres-Isea
Department of Physics, University of Michigan

The objective of this project is to develop a detector which possesses the spatial properties of a position sensitive double sided scintillator detector and the enhanced spectral and pulse shape discrimination properties of a deuterated scintillators. A characterization study was conducted at the Michigan Ion Beam Laboratory (MIBL) using the d(d,n) reaction as a source of neutrons. The d(d,n) reaction was chosen because of the emission of a single monoenergic neutron group and favorable kinetic energy shift with angle, which overlaps the region of interest for this study. Preliminary results indicate 2.5 cm spatial resolution for En ~1-5 MeV. Data analysis for the MIBL measurement is in process.

This work is funded by the National Science Foundation (NSF, PHY0969456).

Horizontal view of the assembled 5 cm dia. x 33 cm position sensitive detector deuterated liquid scintillator detector (left). An axial view of the double sided cell under UV illumination (right). The inert gas bubble can be seen as the flat strip in the axial view. A 30 cm white scale is shown for reference.

BISMUTH SURFACTANT GROWTH OF $INAS_{1-X}S\ B_X$ ALLOYS

E.M. Anderson[1], W.L. Sarney[2], S.P. Svensson[2], J.M. Millunchick[1]
[1]Department of Materials Science and Engineering, University of Michigan
[2]Army Research Laboratory, Adelphi, MD

Thin InAsSb films were grown on top of GaSb via molecular beam epitaxy at 385, 405, and 415 ˚C with varying bismuth fluxes at both ARL and UM. Rutherford Backscattering Spectrometry (RBS) was used at MIBL identify any Bi incorporation into the InAsSb films. The Bi edge would be expected at approximately channel 1740, but was not present as apparent in the figures below. The edge at approximately channel 1620 corresponds to the In and Sb in the film, the edge at approximately channel 1500 corresponds to the As in the film, while features at lower channels are a result of the film thickness and overlapping signals from the film and the GaSb substrate. The films grown at 385 ˚C show that the InAsSb films are compositionally homogeneous, as indicated by the plateaus in the spectra. The films grown at 405 and 415 ˚C show evidence of compositional inhomogeneity, as indicated by the rounded-off and peaky features. This is being further investigated by high resolution x-ray diffraction.

JMM, EMA, and CP gratefully acknowledge Chakrapani Varanasi and the support of the Department of Defense, Army Research Office via the grant number W911NF-12-1-0338.

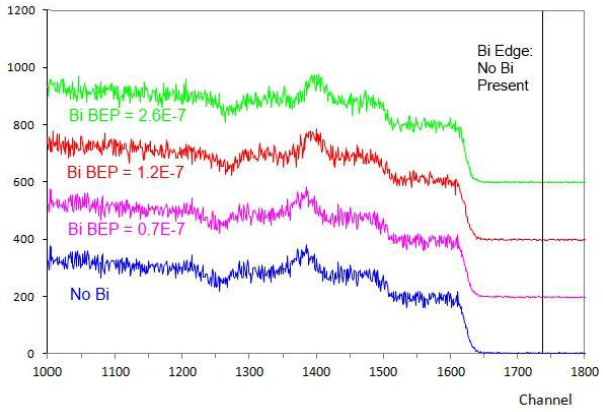

RBS spectra of samples grown at 385˚C. All of the samples show a plateau, which is characteristic of a homogeneous film. No evidence of incorporated Bi was found.

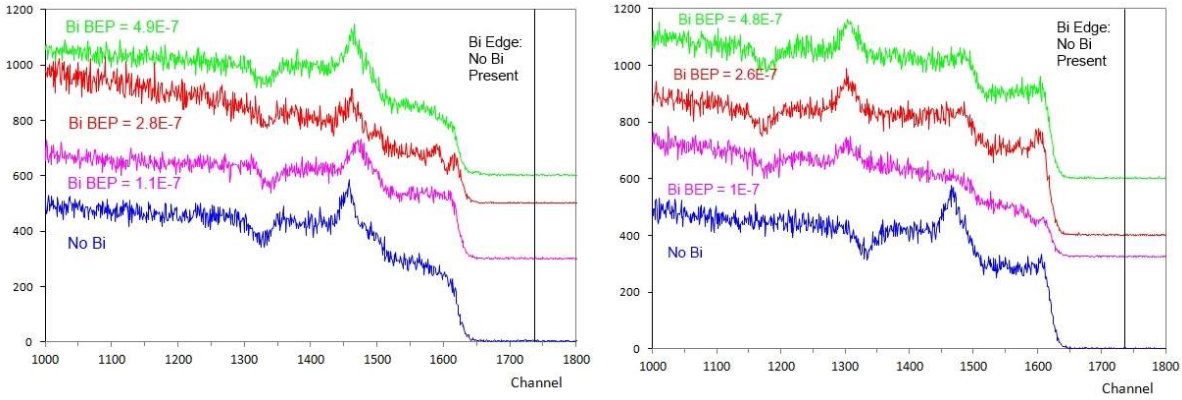

RBS spectra of samples grown at 405 ˚C (left) and 415˚C (right). Only the samples grown 1.1 x 10^{-7} torr Bi BEP at 405 ˚C and the sample grown without Bi at 415˚C show a plateaus, which is characteristic of a homogeneous film. The other films have varying features indicating compositional inhomogeneities. None of the films showed evidence of Bi incorporation at these temperatures.

BISMUTH INCORPORATION IN GaAsBi FILMS GROWN BY MOLECULAR BEAM EPITAXY

R.L. Field III[1,2], T. Jen[2], J. Occena[2], B. Yarlagadda[2], C. Kurdak[1], R. S. Goldman[1,2]
[1]Department of Physics, University of Michigan
[2]Department of Materials Science and Engineering, University of Michigan

Due to their significant energy band gap bowing, dilute bismide compound semiconductor alloys can be grown with a range of band gap energies while maintaining near lattice matching with common substrates. Thus, GaAsBi alloys are promising candidates for a wide range of applications, including long-wavelength light-emitters and detectors, high-performance electronic devices, and high efficiency solar cells. To date, the relationship between Bi incorporation mechanisms and the electronic and optical properties of GaAsBi alloys is not well understood. Therefore, we have investigated the influence of Bi incorporation on the electronic properties of GaAsBi using Si as both an *n*-type and *p*-type dopant. For our studies, we grow GaAsBi alloy films by molecular beam epitaxy. To estimate the bismuth composition in the films, we use a combination of high-resolution X-ray diffraction (HRXRD) and Rutherford backscattering spectroscopy (RBS). As shown in the figure, RBS was performed to determine Bi composition in conjunction with NRA (SIMNRA) code, from which a Bi composition vs. HRXRD peak separation calibration curve was extracted. This allows us to determine Bi composition for additional GaAsBi films from HRXRD measurements.

We gratefully acknowledge the support of the National Science Foundation through Grant DMR-1006835.

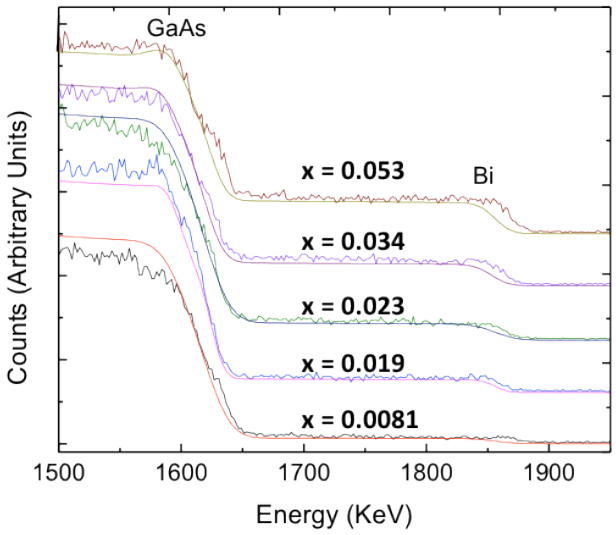

RBS spectra for $GaAs_{1-x}Bi_x$ films of various Bi composition, *x*. The Bi composition was determined using NRA (SIMNRA) code.

HEAT EXCHANGER FOULING IN THE FOOD PROCESSING INDUSTRY

L. Moresco, J. Youngsman
Boise State University

Heat exchanger fouling is an issue faced by liquid and solid processing plants from biofuels and petrochemicals, to milk and sugars. Agricultural production, food processing and packaging consumes approximately 70 million BTU per capita in the US. Food processing alone consumes 3% ($3x10^{15}$BTU) of the total energy consumed in the US.

The food processing industry has unique issues when recovering energy from fluid and gas streams which contain organic solids comprised of sugars, fats, starches, and proteins as well as the typical fouling issues related to inorganic deposits in heat exchangers. Organic materials can scald and stick to heat exchanger surfaces rather quickly. Fouling progresses until the heat exchanger must be taken offline (if there are redundant systems) or a complete system shut down for cleaning in a few days (to weeks). Food safety and eliminating contamination uniquely impact food processing. Fouling deposits in food processing heat exchangers can also provide areas for microbial growth.

The goal of this research is to develop a stable modified heat exchanger surface in combination with initiated turbulent flows that will neither harm the quality nor contaminate the processed food. The net result will either prevent or dramatically increase the period between required fouled heat exchanger surface cleaning cycles.

Stainless steel samples have been implanted with F^- atoms at the UM Ion Beam Laboratory in order to modify the surface energy of the sheet. The goal in this particular sample is to create a super hydrophobic surface.

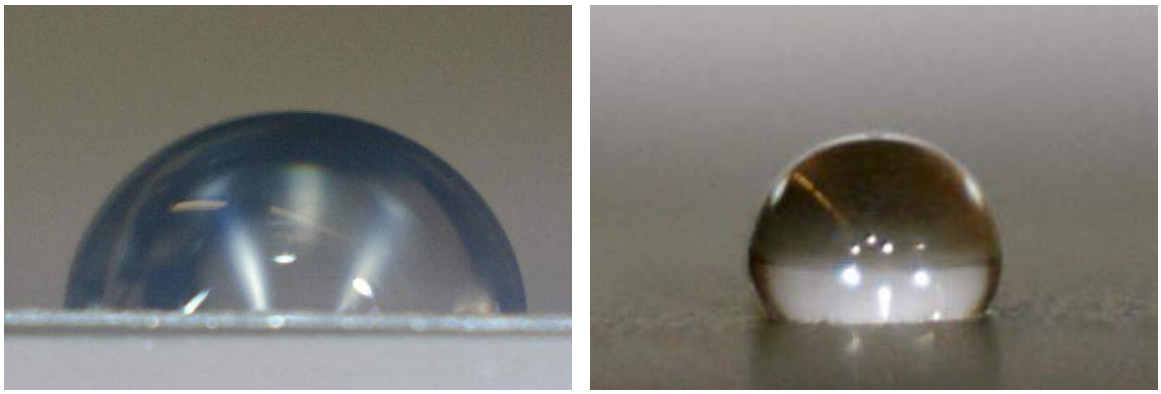

Images of plain 304 stainless steel (left) and surface modified 304 stainless steel (right) showing an improvement in hydrophobicity through Contact Angle Measurements. Surface modification consisted of etch, passivation and F^- implantation steps.

TRISO-COATED FUEL DURABILITY UNDER EXTREME CONDITIONS

[1]I. Reimanis, [2]D. Butt, [2]J. Youngsman, [2]D. Osterberg, [1]Brian Gorman
[1]Colorado School of Mines
[2]Boise State University

The study examines the effect of CO-CO_2 environments on the oxidation behavior of the SiC layer of a TRISO particle and the resulting change in mechanical performance. Corrosion of the carbide layer can occur in the presence of a number of species produced during reactor fission events. Some of these products are seen to diffuse through the carbide layer. Diffusion studies are used to aid in a thorough understanding of the kinetic behavior of the system.

Presently, the diffusion work consists of ion implanted substrates (accomplished at the Michigan Ion Beam Laboratory) of cesium and palladium that are subjected to various heat treatments that vary dwell time and temperature. Analysis is accomplished with SIMS at the Micron Surface Analysis Lab. Additional analyses of structure is conducted with the TEM, SEM, and XPS instruments that are part of the Boise State Center for Materials Characterization. Mechanical testing is completed at the Colorado School of Mines facility.

Results showing improved retention of Cs in the SiC substrate for samples subjected to heat treatments at 750°C for 10 hours. Loss of Cs occurs due to implant damage which causes short circuit pathways. Recrystallization of the substrates improves retention of Cs in the SiC which improves diffusion data collection.

This work is supported by the Department of Energy under NEUP award number DE-AC07-05ID14517, project number 09-257

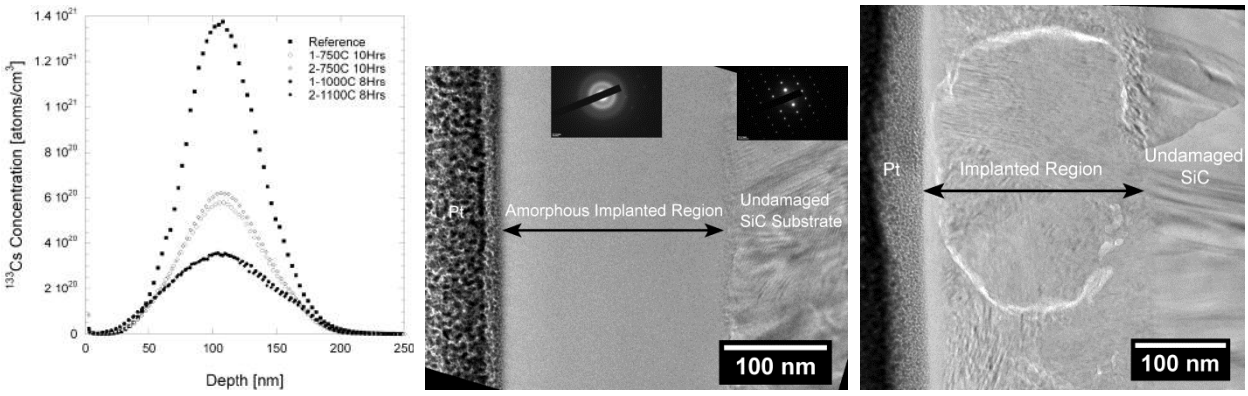

Left: SIMS concentration profiles of two Cs implanted SiC samples showing the as-implanted profile (Reference) compared to replicates of the profiles after recrystallization at 750°C for 10 hours, and after annealing of the recrystallized samples at 1000 and 1100°C for 8 hours.

Middle: A transmission electron microscopy image and selected area diffraction patterns of a Cs-implanted SiC sample illustrating the extent of the amorphous region generated due to ion implantation.

Right: A transmission electron microscopy image of a typical recrystallized region in an annealed sample showing a large grain, a portion of which shares the same orientation as that of the undamaged, underlying Sic substrate after annealing at 775°C for 6 hours.

UNDERSTANDING AG TRANSPORT IN SIC AND C+ IRRADIATED SIC

T.J. Gerczak, I. Szlufarska, B. Leng
Materials Science Program, University of Wisconsin

Release of Ag from intact TRISO coated particle fuel has been a phenomenon of interest to nuclear fuel developers from the inception of the fuel design. In the TRISO fuel design, the SiC layer serves as the primary barrier to select metallic fission products not stabilized in the fuel kernel. Transport across the SiC layer is expected to be the rate-limiting step in Ag release and is hypothesized to be due to a diffusional process. Diffusion coefficients have been observed to vary orders of magnitude from surrogate experimental observations and those from post irradiation examination of TRISO fuel. As such it is assumed irradiation effects may modify the SiC microstructure and promote accelerated transport. This work serves to investigate the role of irradiation on Ag transport in SiC focusing on as-received SiC substrates and C^+ irradiated SiC substrates and will utilize ion implantation to fabricate diffusion couples.

This work consists of a two series investigation of Ag transport in as-received SiC and C^+ irradiated SiC. In both case the same polycrystalline SiC substrates will be implanted with 400 keV Ag^+ ions at 300°C to doses of $1x10^{14}$ Ag^+/cm^2 and $5x10^{14}$ Ag^+/cm^2 in the 400 kV implanter at the University of Michigan Ion Beam Laboratory. The near Gaussian Ag implantation peak serves as constant buried Ag source for high temperature diffusion analysis up to ~1625°C. After implantation the SiC substrates are exposed to high temperature to drive thermal transport. The as-received substrates were implanted and fully characterized.

The change in Ag distribution was measured by secondary ion mass spectroscopy (SIMS) by the ICTAS at Va. Tech using a CAMECA IMS 7f Geo. Ag redistribution was observed in the primary implantation peak as well as Ag concentration "tail" extending into the bulk past the implantation peak. The observation of the Ag concentration "tail" confirms a thermal diffusion process contributes to Ag transport in polycrystalline SiC. Transport in an irradiated substrate will be understood following thermal exposure and SIMS analysis of the C^+ irradiated and Ag^+ implanted diffusion couples.

This work is supported by the US DOE, Office of Nuclear Energy Nuclear Energy University Program (NEUP), award number 11-2988, and by the US DOE, Office of Nuclear Energy under DOE Idaho Operations Office Contract DE-AC07-051D14517, as part of an ATR-NSUF experiment.

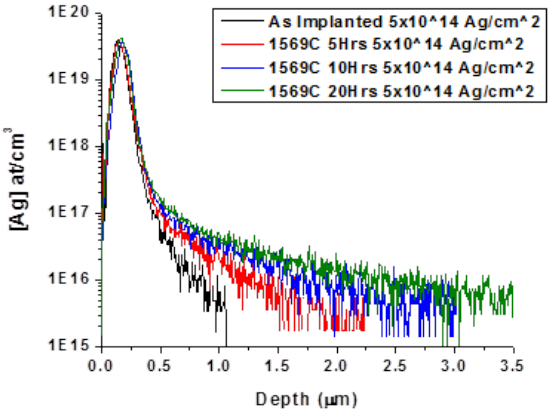

SIMS Ag depth profile for $5x10^{14}$ Ag^+/cm^2 implanted in polycrystalline-SiC and exposed to 1569°C 5-20 hours to drive thermal diffusion.

STABILITY OF PRECIPITATES UNDER ION IRRADIATION

L. Tan[1], G.S. Was[2]
[1]Materials Science and Technology Division, Oak Ridge National Laboratory
[2]Department of Nuclear Engineering and Radiological Sciences, University of Michigan

Different MX precipitates have been used in ferritic-martensitic (FM) steels as strengthening elements. Recently, TaC precipitates were observed unstable under Fe^{3+} ion irradiation at 500°C. The objective of this study is using Fe^{2+} ion irradiation to evaluate the stability of TaC, TaN, and VN nanoprecipitates. The outcome of this study would help not only understanding the degradation mechanisms of current reduced-activation and conventional FM steels but also developing advanced radiation resistant alloys.

Three ferritic model alloys were fabricated to favor the formation of TaC, TaN, and VN nanoprecipitates, respectively. Mini-bars (2x2x20 mm^3) were machined from the alloys with one of the longitudinal surfaces polished to mirror-finish for 5 MeV Fe^{2+} ion irradiation at 500°C, using the Michigan Ion Beam Laboratory (MIBL) through the ATR-NSUF. The microstructures of the irradiated mini-bars were characterized at ORNL using TEM/STEM. The FIB lift-out TEM specimens, parallel to the irradiation direction, provided an overall picture of the MX evolution as a function of the irradiation depth with low dose at surface to damage peak and then into bulk matrix without irradiation. The following figure shows an example using VN.

The characterized results indicate that the nanoprecipitates are non-stoichiometric. The irradiation did not alter their crystallinity, but may have changed their defect structures. Statistic analyses of the particle size and density as a function of depth and irradiation dose indicate that irradiation resulted in slight dissolution and moderate reprecipitation of TaC, which is in contrary to the reported complete dissolution of TaC under similar irradiation condition. Unlike TaC, significant dissolution was observed for TaN. However, VN had moderate growth. Detailed description and discussion are presented at an international conference and reported in peer-reviewed journal articles.

This work is supported by the U.S. Department of Energy under contract DE-AC05-00OR22725 with UT-Battelle, LLC. Dr. O. Toader of MIBL conducted the ion irradiation experiments and Mrs. D.W. Coffey or ORNL prepared the FIB-TEM specimens.

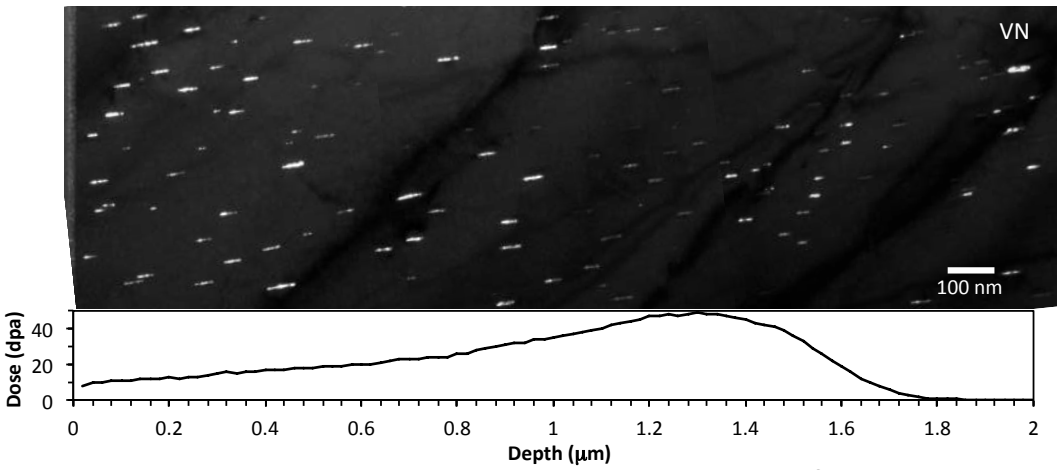

Dark-field image showing the evolution of VN precipitates (white) under Fe^{2+} irradiation at 500°C from the irradiated surface (left), experiencing increased dose as shown in the SRIM simulated depth-dependent irradiation dose profile beneath the image, to bulk matrix without irradiation (right).

EFFECT OF RADIATION AND TEMPERATURE ON STABILITY OF OXIDE NANOCLUSTERS IN ODS STEELS

J. He, K. Sridharan
Department of Nuclear Engineering and Engineering Physics, University of Wisconsin

Oxide dispersion strengthened (ODS) steels are being actively considered as materials for fuel cladding for next generation of fission reactors. ODS steels have a fine nanaometer size scale yttrium/titanium oxide particles dispersed in a ferritic matrix and are produced by mechanical alloying (MA) of the initial powders followed by consolidation by hot isostatic pressing (HIP) or hot extrusion. ODS steels have superior creep rupture strength compared to conventional ferritic steels due to the nano-scale oxide particles in the matrix which impede dislocation movement. At the same time they provide the higher swelling resistance inherent to ferritic steels. Furthermore, the nanoparticles in the ODS steel improve radiation resistance by acting as sinks for helium and point defects that form during irradiation. The chemical and morphological stability of the oxide nanoparticles under radiation is crucial to the expected superior performance of ODS steels.

In this research, the synergistic effects of helium implantation, irradiation, and temperature on the stability of nanoclusters (oxide nanoparticles) in 14YWT ODS ferritic steel have been systematically studied using the atomic probe tomography (APT) technique. The APT technique allows for successful imaging of nanoclusters smaller than 2 nm and provides for high spatial resolution and excellent elemental identification capabilities. More importantly, APT provides a direct three-dimensional reconstruction of nanoclusters on an atomic scale, allowing for the accurate determination of the composition of both nanoclusters and matrix. A realistic assessment of radiation damage in ODS steels can be achieved by defect creation in the presence of helium. Therefore, helium was implanted into the ODS steel at room temperature using 270KeVand 200KeV energies to achieve a uniform concentration (2000appm) of helium below the surface. This implantation was performed at the University of Michigan's Ion Beam Laboratory. The helium implanted samples were irradiated with 5MeV Ni ions at 300℃, 450℃ , and 600℃ to high dose of 100dpa. A high number density of nanoclusters with enrichment of titanium, oxygen, and yttrium are observed in samples irradiated at the three temperatures. The average size distribution and nanoclusters density for each condition are shown in the figure. The average Guinier radii, <Rg> of the 300℃, 450℃ and 600℃ samples are 1.02, 0.96 and 1.03 nm, respectively, and number densities, Nv were 10×10^{23}, $10\times10^{23}$and $6.7\times10^{23}/m^3$, respectively, indicating that the nanoclusters were not significantly affect by irradiation.

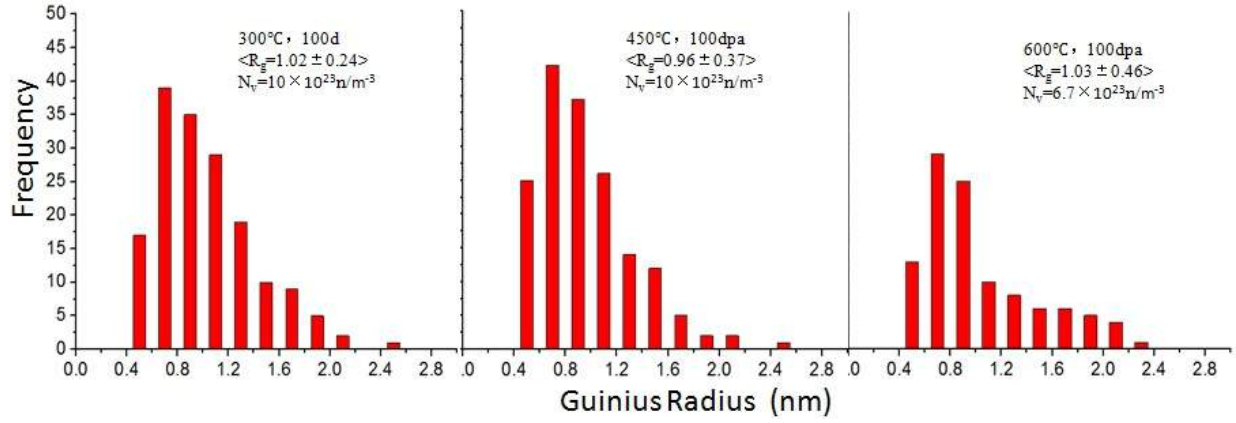

Nanoclusters size distribution of the samples irradiated at 300℃, 450℃ and 600℃, respectively.

THE INFLUENCE OF H^+ IMPLANTATION TEMPERATURE ON EXFOLIATION OF 4H-SiC FILMS

V. P. Amarasinghe[1,2,3], L. Wielunski[1,3], A. Barcz[5], L. C. Feldman[1,2,3], G. K. Celler[1,2]
[1]Institute for Advanced Materials, Devices, and Nanotechnology (IAMDN), Rutgers University
[2]Department of Materials Science and Engineering, Rutgers University
[3]Department of Physics, Rutgers University
[4]Department of Chemistry, Rutgers University
[5]Institute of Electron Technology/Institute of Physics PAS, Warsaw, Poland.

Implantation of 6×10^{16} cm^{-2} H^+ into 4H-SiC causes formation of nanovoids and microcracks under the surface, at a depth corresponding roughly to the implantation range and, after a subsequent annealing at elevated temperatures, these defects lead to exfoliation (and with suitable preprocessing to a layer transfer to a new substrate).

In this study we have investigated the dependence of surface blistering (indicative of favorable conditions for exfoliation) of 4H-SiC on implantation temperature in the range from 77K to 873K. All samples were implanted at 180 keV (R_p= 1.07 μm) with a dose of 6×10^{16} H^+ cm^{-2} (for comparison one sample received a lower dose of 3×10^{16} H^+ cm^{-2}). To characterize damage distribution in implanted samples we utilized ion channeling with 2.4 MeV He ions (Fig. 1). It is clear that the radiation damage peak is highest for the liquid nitrogen cooled implant at -196°C, and decreases monotonically with the implant temperature going up. This is consistent with dynamic self-annealing of point defects already during the implantation, the rate of such annealing increasing with temperature. Arrhenius plots, in Fig. 2, show approximately the same activation energy, $E_a \cong 3.6$ eV, for all implant temperatures. Surprisingly, the required thermal budget for blistering has a maximum for the sample implanted at T=35°C, with both higher and lower temperatures requiring less annealing. The current hypothesis is that at 35°C some defects are eliminated by dynamic annealing while H atoms are not mobile enough to agglomerate. The net result is less residual implantation damage as compared to -196°C implant, but also less agglomeration as compared to a 300°C "hot" implant.

This work has been partially supported by the Semiconductor Research Corporation (SRC) through GRC task 2166.001.

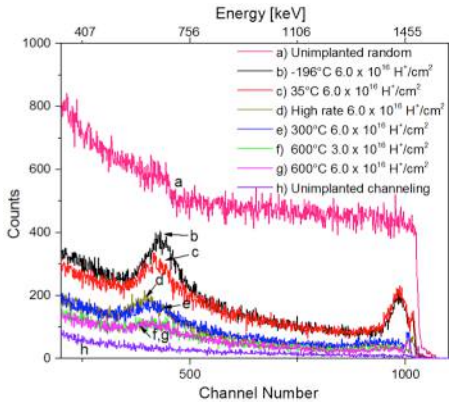

Fig. 1. Ion channeling data.

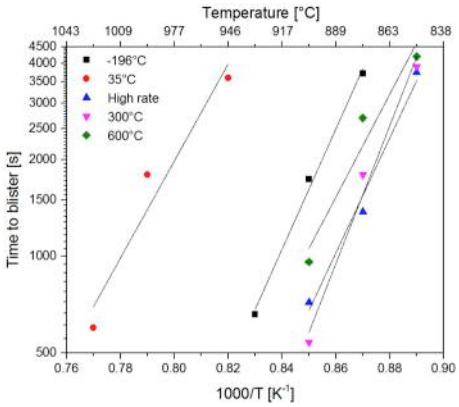

Fig. 2. Arrhenius plots for surface blistering at different implant temperatures. ("High rate" appears equivalent to ~250°C)

SIMS STUDY OF SODIUM DIFFUSION IN $Cu(In_xGa_{1-x})Se_2$

T. Erickson, P. Tsai, A. Rockett
Department of Materials Science and Engineering, University of Illinois

For this work we grew epitaxial thin films of $CuInSe_2$ (CIS), $CuGaSe_2$ (CGS) and $CuInGaSe_2$ (CIGS) with minimal quantities of sodium. CIGS and related chalcopyrite materials have attracted attention for potential applications in thin film solar cell absorber materials. These materials show good electronic properties in polycrystalline films, in which sodium has been shown to have a significant impact. Epitaxial films were used to study the effects of sodium on bulk crystals without the influence of grain boundaries. The films were then annealed in the presence of sodium fluoride for various times and at various temperatures.

The thin films were grown on GaAs with a hybrid co-sputtering system, using separate copper, indium and copper gallium alloy targets, with a selenium effusion cell. The film stoichiometry was controlled through varying the currents to the magnetrons currents, along with an overpressure of Se in the chamber. The anneals were carried out in tube furnace with dry nitrogen. Times were varied from 10 minutes to 1 hour, and temperatures from 400°C to 600°C.

Secondary Ion Mass Spectroscopy (SIMS) analysis was used to determine how quickly and at what temperatures sodium diffused through bulk CIGS crystals, as well as effecting diffusion of other species, especially gallium. Some unannealed samples were implanted at MIBL with sodium at an energy of 300 keV, and a density of $5x10^{15}$ cm^{-2}. SIMS was performed on the implanted samples to calibrate the signal levels from the annealed samples, to allow for quantifying the sodium content of the films.

We gratefully acknowledge the support of the U.S. Department of Energy Office of Energy Efficiency and Renewable Energy under contract DE-EE0005405.

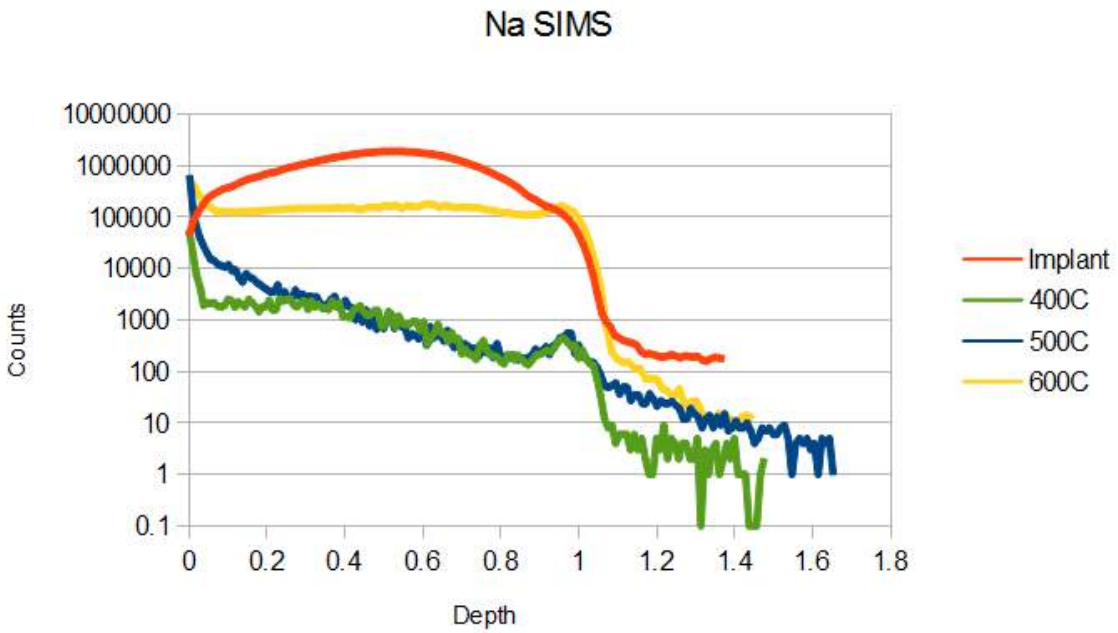

Sodium SIMS profiles from the ion implant performed at MIBL, and 3 annealed samples. Samples were annealed for 10 minutes at the listed temperatures.

OBSERVATION OF CHROMATE AND MOLYBDATE AIDED REPASSIVATION AND INHIBITION OF HYDROGEN UPTAKE IN AA7075-T6

S.B. Madden, J.R. Scully
Center for Electrochemical Science and Engineering, MSE, University of Virginia

The objective of the research presented is to understand inhibitor assisted repassivation of high strength aluminum 2000 and 7000-series alloys in aqueous environments rich in aggressive halides. Introduction of chromate and molybdate to full immersion environmental fatigue crack propagation (EFCP) tests have shown that these inhibitors are capable of retarding the growth rate of cracks and that this inhibition is inhibitor concentration dependent. We examine the potential of chromate, molybdate and other selected inhibitors to form or aid in stabilization of protective surface oxides in harsh crack tip environments. This will lead to greater understanding of the mechanisms through which inhibitors can effect static and cyclic crack growth.

Crack tip film rupture events are thought to lead to hydrogen embrittlement and/or anodic dissolution in the crack tip. The ability of a stable passive film to regrow after film rupture is thought to be critical because it reduces the production of atomic hydrogen at the crack tip by limiting dissolution, hydrolysis of metal ions, and coupled proton reduction. One theory is that the Al_2O_3 oxide is also a hydrogen permeation barrier which limits hydrogen ingress. The reduction in atomic hydrogen on the surface of the metal and the presence of a permeation barrier decreases the amount of embrittling absorbed atomic hydrogen in the fracture process zone and slows anodic dissolution of Al. Although this theory is consistent with frequency dependence of fatigue damage, experimental proof of such inhibitor function is lacking.

One centimeter square samples of 1.5 mm thick AA7075-T6 samples were ground to 800 grit with SiC grinding paper while submerged in 1 M chloride solution with and without the addition of selected corrosion inhibitors and held potentiostatically for 1 h at -0.8 V (SCE). RBS and ERD analysis of the resulting oxide chemistry and thickness as well as hydrogen depth profiles were conducted and are reported below. Formation of a thin chromate rich oxide film reduced the hydrogen absorption into the substrate. Formation of a thick molybdenum oxide film was observed. However, the reduction in hydrogen uptake was not observed indicating that the film was not an effective barrier to hydrogen ingress compared to chromate.

This work is supported under SERDP project number WP-1621 and the DoD TCC.

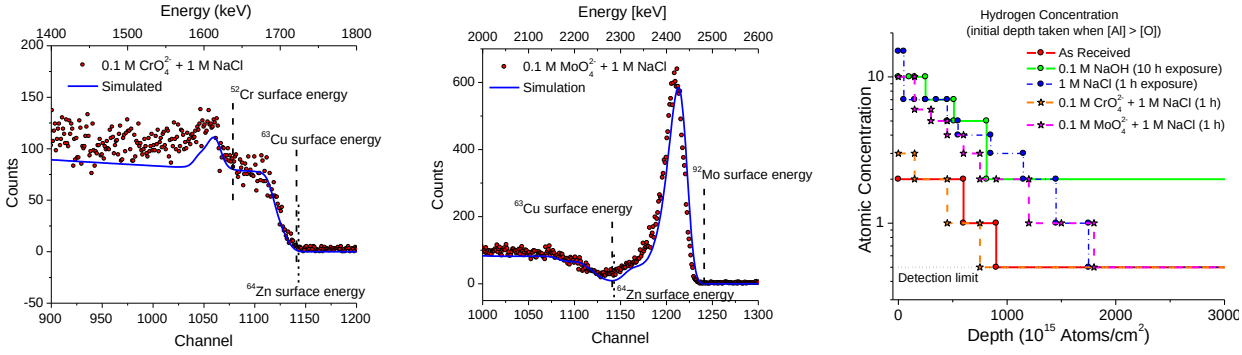

RBS showing chrome and molybdenum rich oxide layer on AA7075-T6 and analysis of ERD hydrogen depth profile showing decrease in concentration when abrasion is conducted in the presence of CrO_4^{2-}.

EVALUATION TECHNOLOGY OF IRRADIATION INDUCED DEGRADATION IN REACTOR INTERNALS OF PWRS

S.S. Hwang, H.P. Kim, Y.S. Lim, D.J. Kim, S.W. Kim, M.J. Choi, M.K. Jung,
S.R. Lee, J.H. Kwon, H.H. Jin, C.S. Yoo, H.O. Lee, M.J. Hwang
Nuclear Materials Division, Korea Atomic Energy Research Institute

As long term operation of a nuclear power plant over 30 years, the problems of irradiation-induced degradation such as an IASCC (Irradiation Assisted Stress Corrosion Cracking), a swelling and a hardening have been reported in several reactor internals. For the development of the IASCC management technology, we evaluated the characteristics of microstructure, the mechanical properties in a small scale and the IASCC sensitivities using the proton irradiated specimens which have the irradiation doses of 1, 3, 5 and 10 dpa.

The microstructure observation of proton irradiated SS316 specimens using TEM, shows angular shaped voids under 10 nm in size distributed all over the specimen irradiated to 1 dpa, and high density of dislocations in the 3 dpa specimen. Plate shape precipitations were distributed all over the specimen of 5 dpa and several micro-twins were observed in the 10 dpa specimen. In the case of non-irradiated specimens, precipitates were not often observed in grains and grain boundaries, and it had a low dislocation density. For the measurement of the mechanical properties in a small scale, we have been performing nanoindentation tests for hardness and elastic modulus and micropillar compression test for tensile properties like yield strength. These tests were to quantify the mechanical properties on irradiated surface which has a small thickness under 20 um.

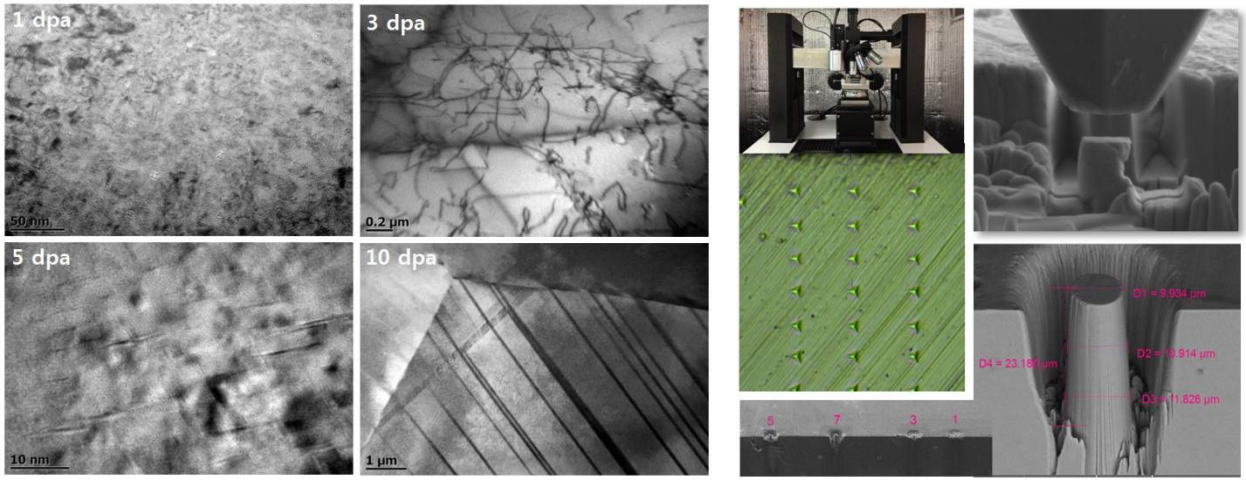

AN INVESTIGATION INTO THE MICROSTRUCTURAL EVOLUTION OF BINARY ZIRCONIUM ALLOYS WHEN SUBJECTED TO PROTON-IRRADIATION

M. Topping, M. McDonagh, M. Preuss
University of Manchester, UK

Zirconium (Zr) alloys are widely used in light water reactors for nuclear fuel assemblies and structural components. The safe operation of these assemblies requires dimensional stability to ensure that both sufficient coolant flow is provided to the fuel rods and that the control rods can be inserted as and when required. However during their operational lifetime these fuel rods are prone to dimensional changes, which can lead to bowing and buckling. This phenomenon is known as irradiation induced growth (IIG).

The main cause of IIG is believed to be dislocation loops that form during irradiation. There are two main types of dislocation loop formed, <a>-loop and <c>-loop dislocations. <a>-loop dislocations form on prismatic planes and have been found to form at low doses, whereas <c>-loops form on the basal plane of the hexagonal close packed (hcp) crystal structure and are only seen at higher doses. It is believed that the <a>-loops are responsible for the initial growth and that the <c>-loops are responsible for the delayed breakaway growth.

Samples at the dpa levels obtained at MIBL (0.5, 1.5 and 3dpa) will allow an investigation into <a>-loop development and a determination of the extent of secondary phase particle amorphization and consequently how this relates to <a> and <c> loop formation under proton irradiation conditions in said Binary Alloys.

It is currently believed that Nb captures diffusing Zr self-interstitials preventing them from their rapid diffusion to form <a> loops and delaying the onset of <c> loop formation and hence irradiation breakaway growth. Fe is a fast diffusing impurity that is exists in the majority of all zirconium alloys, as it is extremely difficult to avoid its inclusion in the processing route. It's presence in the matrix has been modeled and results suggest that it causes vacancies to diffuse faster through the matrix, therefore meaning <c>-loops will form quicker than in the absence of Fe.

To investigate these ideas further a proposal for time at the Diamond Light Source Synchrotron Facility next summer has been approved to investigate the alloys we irradiated in November. Measurement of diffraction patterns with a high enough quality for particle size, volume fraction and anisotropic x-ray line broadening analysis, excellent angular resolution and low background, is achievable using a high-resolution powder diffraction beamline and a multi-analyzing crystal detector. For reliable analysis of dislocation loops, we aim to record over a wide enough range of the diffraction spectrum to include higher order peaks such as the (0004) and (0006) reflections.

Transmission Electron Microscopy (TEM) will also be carried out on the irradiated binary alloys. The aim is to image the dislocation loops and to understand if there are preferential planes they form on. This analytic technique will also allow us to monitor the progress of SPP amorphization/dissolution and provide an understanding of how this affects IIG.

THE BEHAVIOUR OF BINARY Zr-Sn ALLOYS UNDER PROTON IRRADIATION

M. Preuss, A. Harte and T. Seymour
University of Manchester, School of Materials, Manchester, UK

Zirconium (Zr) alloys are utilised for the cladding and structural components of PWR and BWR cores, due to their mechanical and corrosion properties at operating conditions and their low neutron absorption cross section. The deformation behaviour of Zr alloys under irradiation is therefore of considerable interest. However, the nature of such behaviour has proven to be complex and so phenomenological explanations for micro- and macroscopic observations have evolved. In order to optimise the efficiency of reactor cores, a mechanistic understanding of irradiation-induced deformation behaviour of such materials must be developed.

The study of neutron-irradiated material is expensive, time consuming and involves significant radiation hazards. The simulation of neutron-irradiation effects with proton irradiation would decrease the costs and risks associated with handling neutron-irradiated material. However, the question remains as to whether proton-irradiation results in the same effects as neutron-irradiation. Therefore this experiment uses at commercial alloys, Zircaloy-2 and Zirlo®, irradiated to the same doses as neutron-irradiated alloys that we are studying, to provide a direct comparison between the microstructures. We also continue our work on Zr-Sn alloys that was started in 2012 by increasing the dose.

In the present study, recrystallized Zircaloy-2, Zirlo® and binary Zr-Sn alloys with varying concentrations of Sn were irradiated to 2 and 8 dpa for the commercial alloys, and to 5 and 8 dpa for the Zr-Sn alloys at ~350°C with 2 MeV protons at a current of ~30 μA.

Line broadening analysis will be undertaken with X-ray diffraction data to be acquired at the Diamond Light Source synchrotron and complementary analysis will be performed by FEG S(T)EM at the University of Manchester.

SPUTTER TARGET EROSION

J. Amatya
University of Virginia

Sputter deposition is a useful technique for thin film deposition. Sputtering involves the ejection of material from a target source which is then deposited onto a desired substrate. The atoms from the source are ejected due to the interaction of ionized sputtering gas atoms, generally positively charged argon ion, with negatively charged electrode (cathode). There are various types of sputtering methods; the type we use for the deposition of thin films in our system is DC magnetron sputtering technique. In Magnetron Sputtering magnets are placed behind the cathode to trap the free electrons, so that the ionization of the sputtering gas occurs closer to the target aiding in maintaining ionization and sputtering rates at relatively low pressure.

The life of a sputtering target depends upon both the frequency of use and operating power. Additionally, a circular erosion mark or "race track" results from non-uniform sputtering. Knowledge of the depth of the race track is enough to qualitatively analyze the remaining life of a target, but having access to the target without breaking the vacuum is difficult due to the configuration of the target source inside the chamber.

Our target material (silicon) is bonded to a copper cup by indium bonding. For quantitative analysis of our target health, i.e. to determine if we had sputtered through the source target, we prepared a sample of 200 nm thick amorphous Si on top of a Si (100) substrate. A slight trace of indium in the amorphous layer would suggest that the target is worn and needs replacement. We first evaluated our sample with scanning electron microscopy and electron diffraction spectroscopy (SEM/EDS), which did not yield any evidence of indium. As SEM/EDS is a surface analysis technique and less sensitive to low concentration of impurities, we decided to follow up with Rutherford backscattering spectroscopy (RBS) which has a detection sensitivity around 100 ppm. The RBS did not show any indication of indium, suggesting the target is still viable.

We would like to thank Ovidiu Toader and Fabian Naab for their contribution and assistance in the RBS analysis.

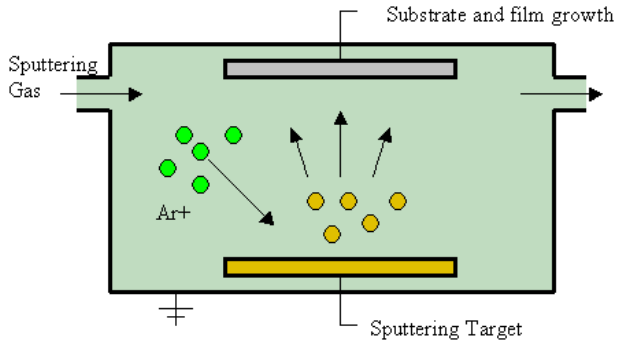

Sputter deposition (from *Wikipedia*)

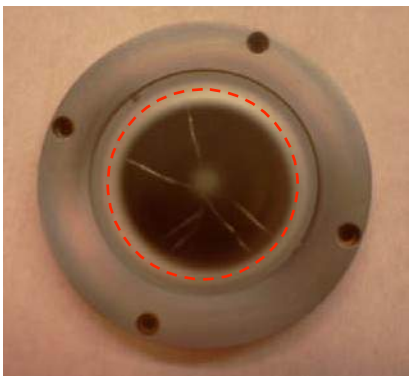

Si sputter target with race rack

RADIATION RESPONSE OF ULTRAFINE GRAINED AUSTENITIC STAINLESS STEELS UNDER Ni ION IRRADIATION AT ELEVATED TEMPERATURES

C. Sun[1] and X. Zhang[2]
[1]Materials Science and Engineering Division, Los Alamos National Laboratory
[2]Department of Materials Science and Engineering, Texas A&M University

The objective of this project is to increase radiation tolerance in austenitic steels through refinement of microstructure. The focus of materials will be on ultrafine grained (UFG) austenitic Fe-14Cr-16Ni alloys and 316L stainless steel. The scientific issues we are trying to address include: (1) High angle grain boundaries can effectively reduce void swelling in these austenitic stainless steels. (2) Radiation hardening in austenitic SSs (at moderate temperature, ~450°C) can be significantly suppressed. (3) Fine grains with high angle grain boundaries are stable against irradiation up to 500°C. The rationale behind these hypotheses is that abundant high angle grain boundaries can be effective sinks for radiation induced point defects and clusters, and thus enhance radiation tolerance.

We obtained UFG Fe-14Cr-16Ni alloy and 316L SS by equal channel angular pressing technique at Texas A&M University. Fig. 1 shows the microstructure of UFG Fe-14Cr-16Ni alloy. Ni ion irradiations at high temperatures were performed at The Michigan Ion Beam Laboratory (MIBL). The irradiated samples and irradiation conditions were listed in the table. Fig. 2 shows an example of the irradiated samples with an irradiated area of 2 × 10 mm. Focused Ion Beam technique was used to prepare thin specimen for transmission electron microscopy (TEM) studies on irradiated samples. The examination of microstructure of irradiated samples under TEM is on the way.

This work is supported by the DOE-NEUP program under contract no. DE-AC07-05ID14517 00088120.

Ni ion irradiation list for Fe-Cr-Ni alloy and 316L stainless steel at MIBL.

Damage level	Energy	Temperature	Samples
100 dpa	5MeV	450°C	Fe-Cr-Ni (AR and 4Bc300), 316L SS (AR and 2Bc300)
	5MeV	500°C	Fe-Cr-Ni (AR and 4Bc300), 316L SS (AR and 2Bc300)
175 dpa	5MeV	450°C	Fe-Cr-Ni (AR and 4Bc300), 316L SS (AR and 2Bc300)
300 dpa	5MeV	500°C	Fe-Cr-Ni (AR and 4Bc300), 316L SS (AR and 2Bc300)

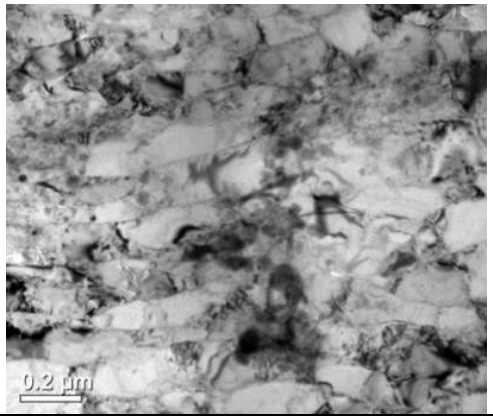

Fig. 1. TEM micrograph of Fe-14Cr-16Ni alloy after ECAE at 300°C for 4 passes (4Bc300). The average grain size is 250 nm.

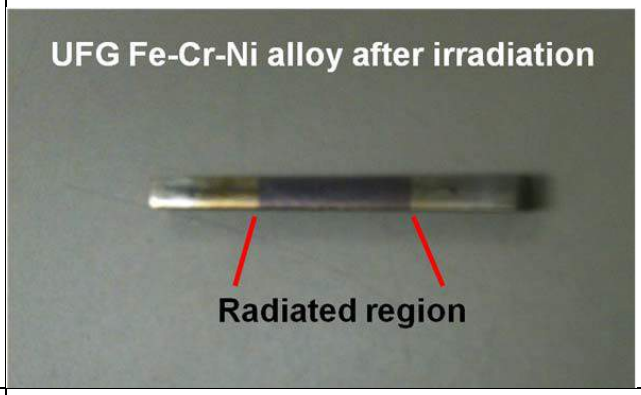

Fig. 2 The UFG Fe-14Cr-16Ni alloy (4Bc300) after Ni ion irradiation to a dose of 175 dpa at 450°C at MIBL.

EVALUATION OF STRESS-CORROSION CRACKING AND MICROSTRUCTURAL CHANGES IN PROTON-IRRADIATED T91, APMT, AND ALLOY 33

Parag Ahmedabadi and Gary S Was
Department of Nuclear Engineering and Radiological Sciences, University of Michigan

Stress corrosion cracking (SCC) and oxidation behavior of ferritic-martensitic alloys T91 & APMT and austenitic Alloy 33 are being evaluated at University of Michigan. This investigation is a part of an ongoing DOE-sponsored project to evaluate ferritic-martensitic alloys as fuel cladding materials for LWR as Accident Tolerant Fuel (ATF). It is well known that in-core stainless steels components are susceptible to irradiation assisted stress corrosion cracking (IASCC) in BWR, hence, it is important to evaluate alloys intend to use in as in-core components such as fuel cladding material.

Three alloys, received from GE, were evaluated for oxidation and SCC behavior (in un-irradiated and proton-irradiated condition) in normal water chemistry (NWC). Three alloys were in rectangular block form viz. APMT (~ 101 x 100 x 30 mm), T91 (~ 64 x 40 x 39 mm), and Alloy 33 (~ 150 x 51 x 16 mm).

To study IASCC behavior and microstructural changes in these alloys due to irradiation, samples of each alloy were irradiated using 2 MeV protons at 360 °C up to 5 dpa. Tensile specimens and TEM bars were irradiated for each alloy; the geometry of tensile specimens and TEM bars is shown in figure at left. Temperatures at various locations on individual specimens during the irradiation were monitored using thermal-imaging camera and the figure at right shows a snapshot taken during the irradiation.

The tensile specimens will be used to evaluate stress corrosion cracking in alloys and TEM bars will be used for microstructural characterization. Specimens will be prepared from the irradiated region on the TEM bars using FIB lift-out technique. The SCC behavior in the irradiated material will be evaluated using tensile specimens in a similar way that was used for the un-irradiated specimen. The strain rate and the level of dissolved oxygen will be kept at the same levels that were used for the un-irradiated specimens. The increase in the yield strength of alloys after irradiation will be estimated from the hardness values in the irradiated region using a small load for hardness measurements.

The work is supported by work supported by the U.S. DOE, National Nuclear Security Administration, under award number DE-NE0000568.

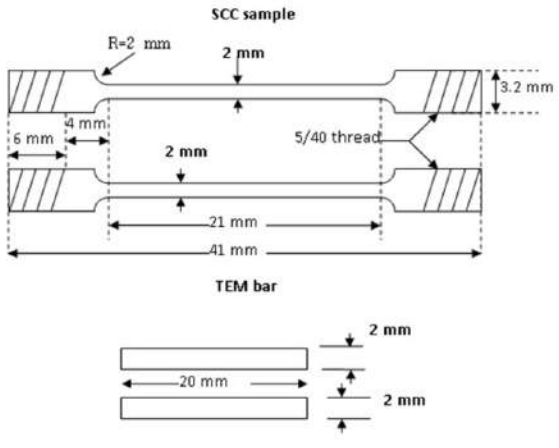

Tensile specimens and TEM bars used for proton irradiation.

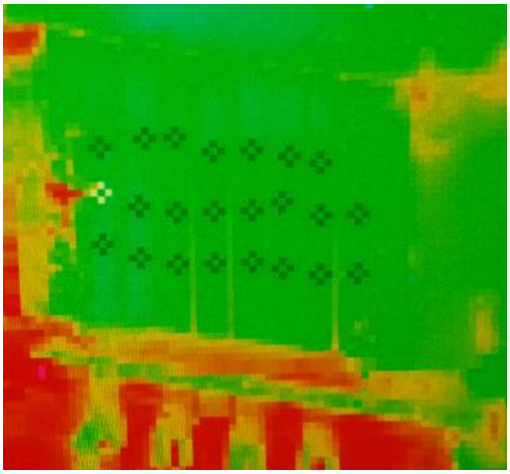

Thermal image of the irradiation stage during proton irradiation.

PROTON-IRRADIATION OF Zr-ALLOY CLADDING COATED WITH DIFFERENT CERAMIC COATING

Parag Ahmedabadi and Gary S Was
Department of Nuclear Engineering and Radiological Sciences, University of Michigan

An integrated research project (IRP) to fabricate and evaluate modified Zircaloy LWR cladding under normal BWR/PWR operation and off-normal events is currently being pursued. This IRP aims at design, fabrication, and performance testing of accident tolerant nuclear fuel cladding. Two approaches toward accident tolerant LWR fuel are adopted based on the modification of existing Zircaloy cladding. The first approach involves application of surface coating on existing Zr-alloy cladding to shift the M+O→MO reaction away from oxide growth during steam exposure at elevated temperature under accident scenario. The second approach is the modification of the bulk cladding composition to promote precipitation of minor phase(s) during fabrication. One of the objectives of the proposed IRP is to evaluate performance of modified cladding material under normal BWR and PWR operation with respect to corrosion, in particular, stress corrosion cracking (SCC) and irradiation-assisted stress corrosion cracking (IASCC).

As a part of this project, Zr-alloy cladding material was given an advance ceramic coating with varying composition of Fe, Cr, and Al. The thickness of the coating was in the range of 500-800 nm. A total of 8 such coated samples were irradiated using 1 MeV protons at 360 °C up to level of approximately ~ 2.3 dpa. The arrangement of the specimens on the Irradiation Stage is shown in figure at left. The range of 1 MeV protons in Zr-alloy is approximately 10 μm, therefore, the entire coating and the coating-substrate interface fall within the region of uniform damage as shown in the figure at right. The damage profile was estimated using SRIM software by summing up energy loss (of incident protons) due to vacancy formation as well as phonons excitations. These specimens will be further tested for the effect of irradiation damage in coating on corrosion behavior in different BWR and PWR environments.

The work is supported by work supported by the U.S. DOE under the NEUP program.

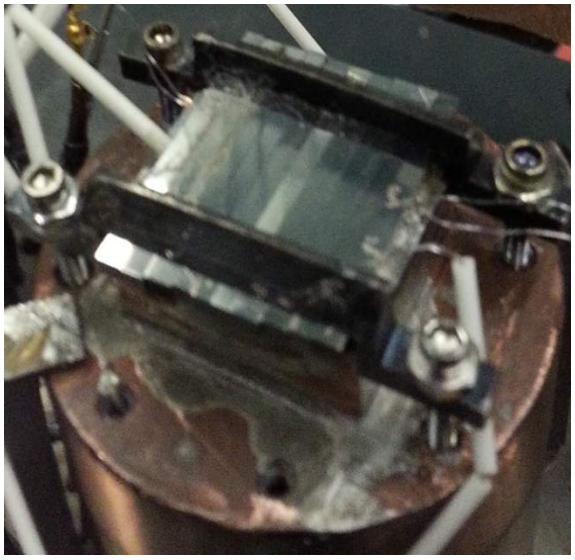

Coated samples loaded on the irradiation stage, prior to irradiation.

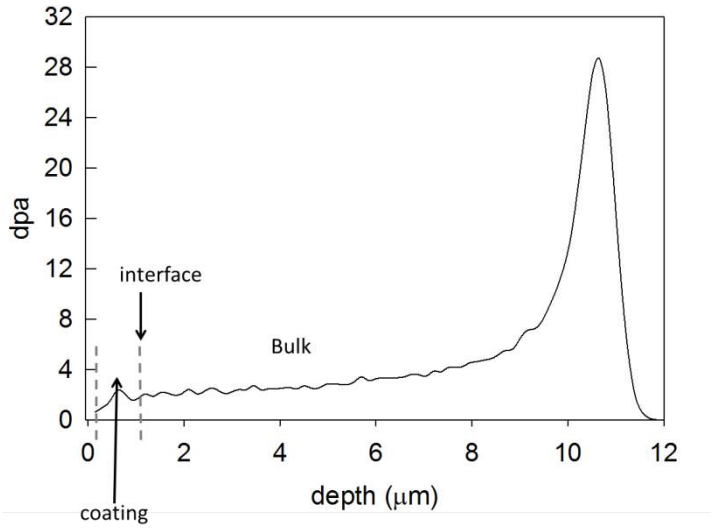

Calculated damage profile (SRIM) for 1 MeV protons in Zr-alloy

CREATION OF NITROGEN VACANCY CENTER IN DIAMOND BY ION BEAM IRRADIATION

R. Barri, J.Q. Xiao
Department of Physics and Astronomy, University of Delaware

When a nitrogen atom replaces one of the carbon atom in diamond crystal, which is adjacent to a vacancy (lack of the carbon atom) in diamond crystal, the Nitrogen Vacancy Center (NVC) has been formed. The ground state of the NVC is a spin triplet state (Quantum Number S=1), which the spin states $m_s=\pm1$ are split (2.87GHz) from the $m_s=0$ in zero magnetic field due to spin-spin interaction. In room temperature the population of electrons in $m_s=\pm1$ is equal the population of electrons in $m_s=0$. If the NVC pumped by 532 nm laser, because of the exceptional electronic structure of the NVC, most of the electrons in $m_s=\pm1$ will end up in $m_s=0$ state, and this is the only quantum polarized state in room temperature. $m_s=\pm1$ is dark state and $m_s=0$ is bright state it means that if an electron is in dark state after being excited by 532 nm laser will come back to $m_s=\pm1$ without emitting fluorescence, while $m_s=0$ is bright state and will come back from excited state by emitting fluorescence radiation.

NVC occurs naturally in both synthetic and natural diamonds. But the concentration of NVC is very low and also they can be in any part of diamond crystal, in scientific research we need to have the NVCs in specific positions inside diamond crystal and also in desired concentration, for doing this we got very high pure diamond crystal (N concentration 5 ppb). Irradiation of the diamond crystal with nitrogen and carbon was conducted (for creating vacancies) in five different parts of diamond with different doses yielding five different concentration of NVC in diamond crystal, which any of them is suitable for different application. We want to use NVC in diamond for following experiments:

Magnetometry: In zero magnetic field, if we apply microwave(2.87 GHz) when we illuminate NVC by 532 nm laser, we will see decrease in fluorescence, because the MW will excite some of the electrons from $m_s=0$, bright state, to $m_s=\pm1$, dark state. In presence of magnetic field, $m_s=+1$ and $m_s=-1$ will separate from each other, also their distance from the $m_s=0$ will change proportional to magnitude of B. Now if we apply 532 nm to NVC and scan the MW frequency we will see decrease in fluorescence in specific MW proportional to B. By using this method 100 PicoTesla sensitivity and 300 nm spatial resolution is achievable.

Detecting Magnetic Nano-Particles: NVC can be used for detecting Magnetic Nano Particles(MNP), for doing this the MNP will be placed close to NVC, then the magnetic field of MNP will cause change in resonance frequency of NVC, by this method the MNP and quantity of them can be detected. For doing this both bulk diamond and nano diamond can be used.

PRELIMINARY STUDY ON IRRADIATION ASSISTED ALKALI-SILICA REACTION IN THE BIOLOGICAL SHIELD BUILDING AND THE REACTOR PRESSURE VESSEL SUPPORT STRUCTURES

Y. Le Pape[1], K. Field[1], C. Mattus[1], O. Toader[2]
[1]Oak Ridge National Laboratory
[2]Department of Nuclear Engineering and Radiological Sciences, University of Michigan

The possibility of a coupling mechanism between irradiation and alkali-silica reaction (ASR) was suggested first by Ichikawa and Koizumi [1]: 2x2 cm^2 a-quartz and amorphous quartz plates were irradiated under a 200 keV Ar ion beam at a dose rate of 6.0 x 10^{12} ions/s·cm^2 (.003 dpa/s) at room temperature. The lattice defect depth was measured between 200 and 300 nm. The critical dose for initiating micro-structural damage was 2.0 x 10^{14} Ar/cm^2 (0.1 dpa) for a-quartz and 0.4 x 10^{14} Ar/cm^2 (0.02 dpa) for amorphous quartz. Full damage was obtained at 6.0 x 10^{14} Ar/cm^2 (0.3 dpa) and 0.6 x 10^{14} Ar/cm^2 (0.03 dpa) respectively. The dissolution rate of the irradiated materials immersed in a 1 mol/L solution of sodium hydroxide was multiplied by more than 20 for a-quartz and approximately tripled for amorphous quartz, hence showing the increased reactivity of aggregate. In a sense, Ichikawa and Koizumi's experiments may have been inspired by ASTM C289-07 aiming at evaluating the potential alkali-silica reactivity of aggregate by a chemical method though no measurement of the alkalinity evolution is proposed.

To demonstrate the possibility of irradiation-assisted ASR (IAASR), further experiments are needed. It is suggested in a first approach to proceed to the irradiation of a-quartz plates (ion beam) in order to develop, just like in Ichikawa and Koizumi's experiments, a superficial amorphous, and hence potentially reactive layer. The damage of the 'plated-aggregate' will be characterized by different observation techniques prior to be put in contact with a high alkaline cement paste. A proof of principle experiment was conducted using the University of Michigan Ion Beam Laboratory's low energy ion implanter. Z-cut single crystal SiO_2 was obtained from MTI Corporation and naturally occurring Opal mineral from Ward Scientific and implanted using Ar^+ ions to a total fluence of 1x10^{14} Ar^+/cm^2 at 400 keV and room temperature. Based on SRIM calculations (Figure at top) the implantation depth should be ~500 nm. A cross sectional focused ion beam lift-out was extracted from the implanted SiO_2 sample to determine the amorphization layer present in the material. The figure shows a bright field TEM image of the implantation surface (in cross-section) and corresponding diffraction patterns. The figure demonstrates the amorphization expected based on known parameters for critical amorphization dose of a-quartz and SRIM calculations were correct. Further characterization, including swelling calculations and IAASR studies, are currently underway at Oak Ridge National Laboratory.

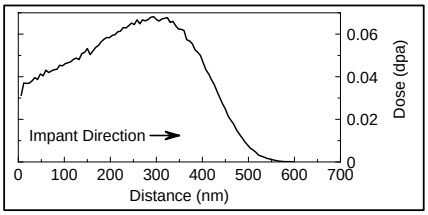

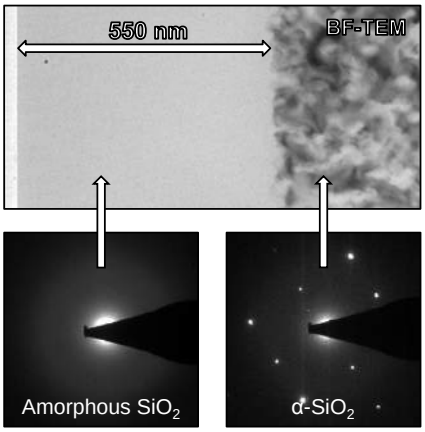

Characterization of an implant completed on α-quartz conducted at the University of Michigan Ion Beam Laboratory for irradiated assisted alkali-silica reaction studies.

SURFACE ENGINEERING OF BULK METALLIC GLASSES TOWARD BIOACTIVITY

W. He, L. Huang
Department of Materials Science and Engineering, University of Tennessee

Bulk metallic glasses (BMGs) are a group of metallic materials with amorphous microstructure, in contract to the ordered crystalline structure of traditional metals or alloys. The unique structure of BMGs results in a combination of material properties including excellent mechanical properties, high corrosion resistance, and good thermal formation capability, which are considered to be suitable for biomedical applications.

The biocompatibility of BMGs has been reported in many studies through *in vitro* cell cultures and primary animal tests. The result in previous studies generally revealed a comparable biocompatibility of BMGs to Ti-alloys. However, the practical use of BMGs as orthopedic implants will not be highly favored at the present due to the lack of bioactivity. In this work, a novel route is designed to impart bioactivity to BMGs by altering their surface properties, using the versatile ion implantation technique.

Ca-ion implantation into the Ti surface was found to enhance the bioactivity of Ti surface. This approach can be extended to improve the bone conductivity of BMGs. The major focus of the current project is to investigate the effects of ion implantation with Ca ions to the bioactivity of Zr-Al-Ni-Cu-Y BMG. As a control, Ar is selected, based on its similarity in the atomic mass to that of Ca, the implantation of which will allow us to distinguish the mechanical effect introduced by ion implantation from the chemical effect associated with Ca-ion implantation.

Ar-ion implantation was conducted in Michigan Ion Beam Laboratory under different settings. *In vitro* cell culture with MC3T3-E1 preosteoblasts was employed to demonstrate ion implantation effect on bone-forming cell responses. High cell viability was observed on all substrates after Ar-ion implantation as shown in the figure below. Qualitatively, numbers of adherent cells varied on different substrates treated under different implantation parameters. Our preliminary results suggest that the cellar responses can be tailored by tuning surface properties via ion implantation.

This work is supported by National Science Foundation under grant CMMI-1100080.

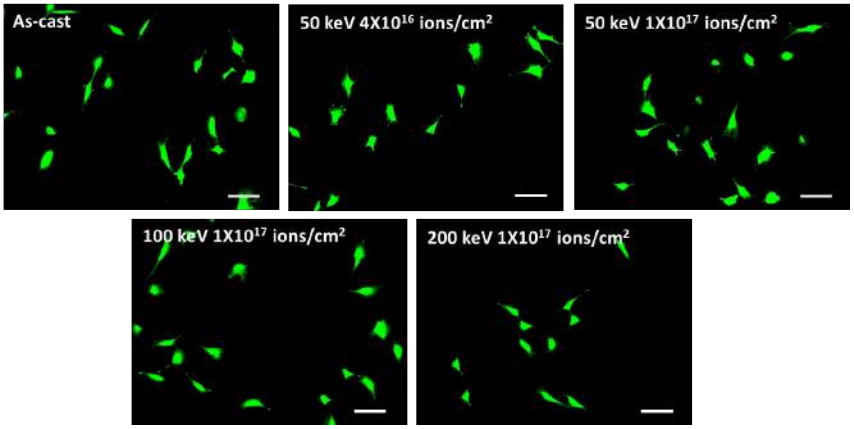

Live/dead staining of MC3T3-E1 mouse pre-osteoblasts on as-cast and Ar-ion implanted $(Zr_{55}Al_{10}Ni_5Cu_{30})_{99}Y_1$ BMGs after 1d growth (Scale: 100 μm).

DETERMINATION OF AREA COVERAGE OF SOLUTION-CAST NANOWIRE NETWORKS USING RUTHERFORD BACKSCATTERING SPECTROMETRY

J. Borchert, K. I. Winey
Department of Materials Science & Engineering, University of Pennsylvania

Transparent conducting materials are an important part of many technologies including touch screens, solar panels, and EM shielding. However, the current material of choice, Indium Tin Oxide, is falling out of favor due to its cost of manufacture and brittle nature. Networks of solution-cast metal nanowires have shown great potential to replace ITO in future devices.

One important property of transparent materials based on nanowire networks is the amount of substrate area covered by nanowires. This quantity has been obtained to some success by various methods in the past including processing of SEM images of nanowire networks and a Finite Difference Time Domain (FDTD) approach relating the optical transmittance of a deposited film to the area coverage.[1] We have worked to develop a new method to more directly measure the content of metal nanowires on a surface using Rutherford Backscattering Spectrometry (RBS).

RBS is typically only suitable for homogenous films of material. Since nanowire networks deposited on a substrate are inherently inhomogeneous, the atomic areal density of the nanowire component element(s) cannot be directly obtained using ion beam data analysis programs such as SIMNRA. We must therefore compare the results from a deposited network to a thin film of the component elements. We can accomplish this using the following relation[2] and recognizing that the experimental parameters, Ω and Q, remain constant.

$$Y_i = \sigma_R(E,\theta)_i \cdot \Omega \cdot Q \cdot (Nt)_i \quad (1)$$

From the data obtained by MIBL we see that the samples with fewer copper nanowires deposited (6A and 7B) on a PET substrate show lower yields of Cu than those with more wires (2A and 2B). This served to validate our method and motivate further experiments which lead to a master's thesis.

Funding for this work was provided by the Laboratory for Research on the Structure of Matter and the University Research Foundation at the University of Pennsylvania.

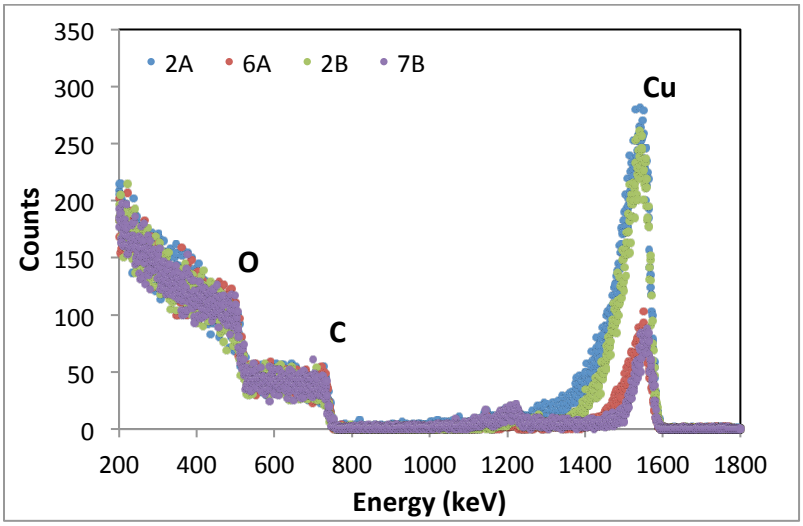

RBS plot of Cu wires on a PET substrate.

RELATIONSHIP BETWEEN LOCAL STRAIN AND SURFACE OXIDE FRACTURE IN PROTON IRRADIATED 316 STAINLESS STEEL

J.A. Duff, F. Scenini, M.G. Burke
Materials Performance Centre, University of Manchester, U.K.

Surface oxide fracture in 316L grade stainless steel in both annealed and 1dpa proton irradiated condition was observed during straining in a Scanning Electron Microscope (SEM). Samples were oxidized for 500 hours in a recirculating autoclave with high purity water at 320°C, 2ppm dissolved hydrogen and 3ppm dissolved lithium as lithium hydroxide. The specimens were then strained inside a FEI Quanta 650 FEG-SEM at room temperature using a Kammwrath & Weiss 5kN microtester. Loading was in approximately 40MPa steps with high resolution images collected at each increment of areas previously mapped by Electron BackScattered Diffraction (EBSD). Digital Image Correlation was then used to determine macro-strain and localized strains.

Both the annealed and proton irradiated sample were loaded to 2.5% strain. While the annealed 316 sample showed only a small number of oxide fractures at grain boundaries, the proton irradiated sample showed extensive oxide fracture along dislocation channels across grains, with transition to adjacent grains also observed.

Project co-funded by the European Commission under the Euratom for Nuclear Research and Training Activities within the Seventh Framework Programme (2007-2011)

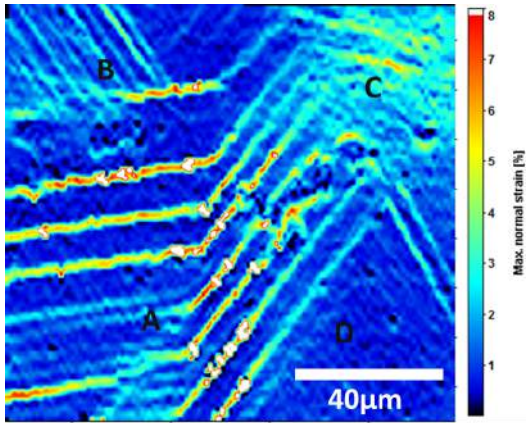

a) DIC calculated surface strain image of 1dpa proton irradiated 316SS stainless steel sample oxidized in high purity water at 320°C and strained in an SEM to 2.5%.

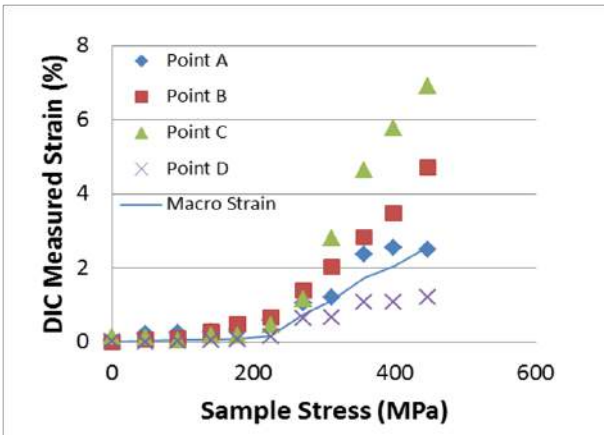

b) Development of strain at locations shown in a).

EFFECT OF BEAM RASTERING ON MICROSTRUCTURE IN FERRITIC-MARTENSITIC STEELS

E.M. Beckett, Z. Jiao, K. Sun, G.S. Was
Department of Nuclear Engineering and Radiological Sciences, University of Michigan

This project studied the effects of beam rastering on at high doses of self- ion irradiation, up to 280 dpa (KP calculation), in HT9 and other ferritic-martensitic (F-M) steels, at 440^{o}C. Of greatest interest is the change in microstructural evolution under irradiation, including void swelling, dislocation loop nucleation and growth, and precipitation.

Self-ion irradiation experiments have been performed on ferritic-martensitic alloy HT9 to determine swelling behavior at 440°C to doses of 280 dpa and above using three different helium implant states. Irradiations were performed on both helium implanted and unimplanted samples using defocused and raster scanning on a Tandetron accelerator at the Michigan Ion Beam Lab. Voids, Ni/Si precipitates and dislocations were examined using transmission electron microscopy (TEM). The raster scanned beam was found to suppress void swelling by suppressing both diameter and number density of the voids, though the effect was strongest in the diameter. A similar trend was found for Ni/Si precipitates, with the diameter and number density suppressed in the raster scanned beam. The loops were smaller in the raster scanned beam, but there was no suppression of the number density. At high dose (280dpa), swelling reached as high as 1.27% in the 10 appm He sample. The results were explained by the Fully Dynamic Rate Theory model. Frenkel pair defects anneal between the pulses from the raster scanning, which decreased supersaturation of vacancies as well as the interstitial population. Since nucleation is a faster process than growth of voids, precipitates and dislocations, rastering had a greater effect on the void/precipitate/dislocation diameter rather than number density, which agreed with the experimental results.

This work is supported by TerraPower, LLC.

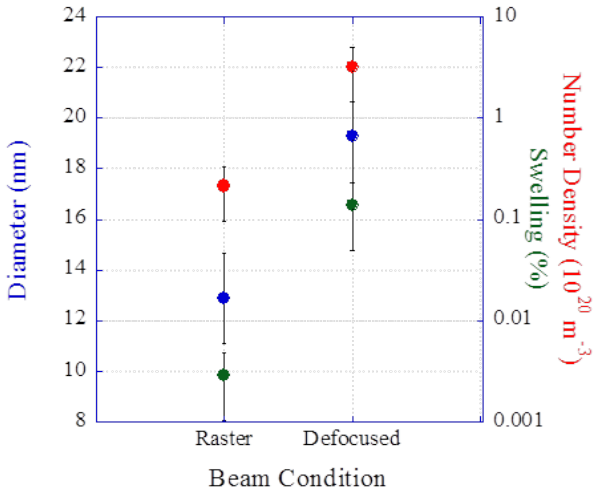

Effect of rastering on voids at 440^{o}C, 140 dpa with 10 appm He.

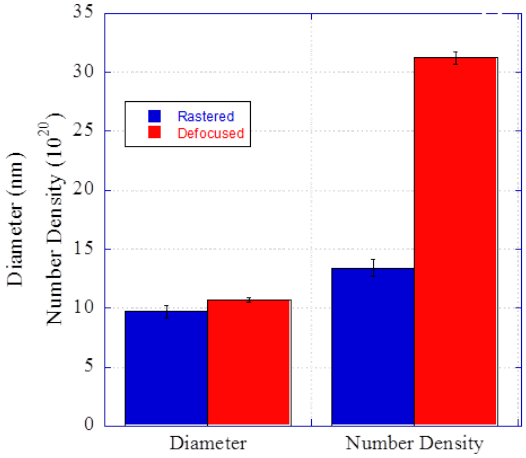

Effect of rastering on Ni/Si precipitates at 440^{o}C, 140 dpa with 100 appm He.

THE EFFECTS OF PROTON IRRADIATION ON THE MICROSTRUCTURAL EVOLUTION OF INCONEL X-750

C.D. Judge[1], G. Was[2], Z. Jiao[2], G.A. Botton[3], M. Griffiths[1]
[1]Atomic Energy of Canada Limited, Chalk River, Ontario, Canada
[2]Department of Nuclear Engineering and Radiological Sciences, University of Michigan
[3]McMaster University, Hamilton, Ontario, Canada

Modern CANDU® reactors employ Inconel X-750 material within the reactor core. The Inconel X-750 material is exposed to two distinct temperature ranges depending on the component configuration of approximately 120-280°C, and 300-330°C. In recent years it has been determined that Inconel X-750 material in CANDU reactors has the potential to lose strength and ductility following irradiation in reactor. The degree of change is a function of fluence and irradiation temperature.

The high thermal flux in a CANDU reactor leads to transmutations in Ni, resulting in high concentrations of He and elevated irradiation damage projected up to 100 dpa and 30000 appm He after 30 years of service. Transmission electron microscopy (TEM) on ex-service material (up to 55 dpa and 18000 appm He) has confirmed the presence of a high density of helium bubbles in the matrix and aligned along grain boundaries. The segregation of helium bubbles to grain boundaries has been identified as the leading mechanism resulting in reduced strength, ductility and inter-granular fracture.

Typical in working with ex-service material, it is difficult to identify how different variables affect the mechanical properties from the available data. Gaps remain in understanding some of the underlying mechanisms resulting in reduced strength and ductility that can be addressed through controlled experiments. A proton irradiation program of Inconel X-750 pre-implanted with helium has been conducted using the Tandetron accelerator at the Michigan Ion Beam Laboratory (MIBL) to supplement the information obtained from ex-service neutron irradiated material. The proton irradiation was not expected to emulate the damage from thermal neutrons, but has been used to complement our current understanding with a controlled experiment. Samples pre-implanted with helium have been irradiated with protons at 380°C in 20 dpa intervals up to 60 dpa with 18000 appm helium.

The microstructural evolution of proton irradiated samples has been characterized with TEM. The image below (centre) shows a TEM lamella prepared with a focused ion beam (FIB) at the Centre of Advanced Energy Studies (CAES) from a sample with 60 dpa and 18000 appm helium. TEM was performed at the Canadian Centre of Electron Microscopy (CCEM) at McMaster University. Electron diffraction and electron energy loss spectroscopy (left) was used to characterize the evolution of secondary precipitates, gamma prime. In all irradiation conditions observed, the gamma prime has not been completely disordered. Fresnel contrast, bright-field, imaging was used to characterize voids and helium bubbles (right). It was observed that large, sparsely dispersed, voids were formed in regions without helium implantation, while helium bubbles having diameters of 1-3 nm where observed in regions containing the implanted helium. The helium bubbles were uniformly distributed within the matrix with some additional segregation to the grain boundaries, similar to ex-service spacers.

The complete characterization of the microstructural evolution from proton irradiated X-750 has provided valuable insights regarding the stability of secondary precipitates, and has given a means of supplementing more costly in-reactor irradiation programs.

This work has been funded by the CANDU Owners Group (COG) Joint Project 4363.

® CANDU is a registered trademark of Atomic Energy of Canada Limited.

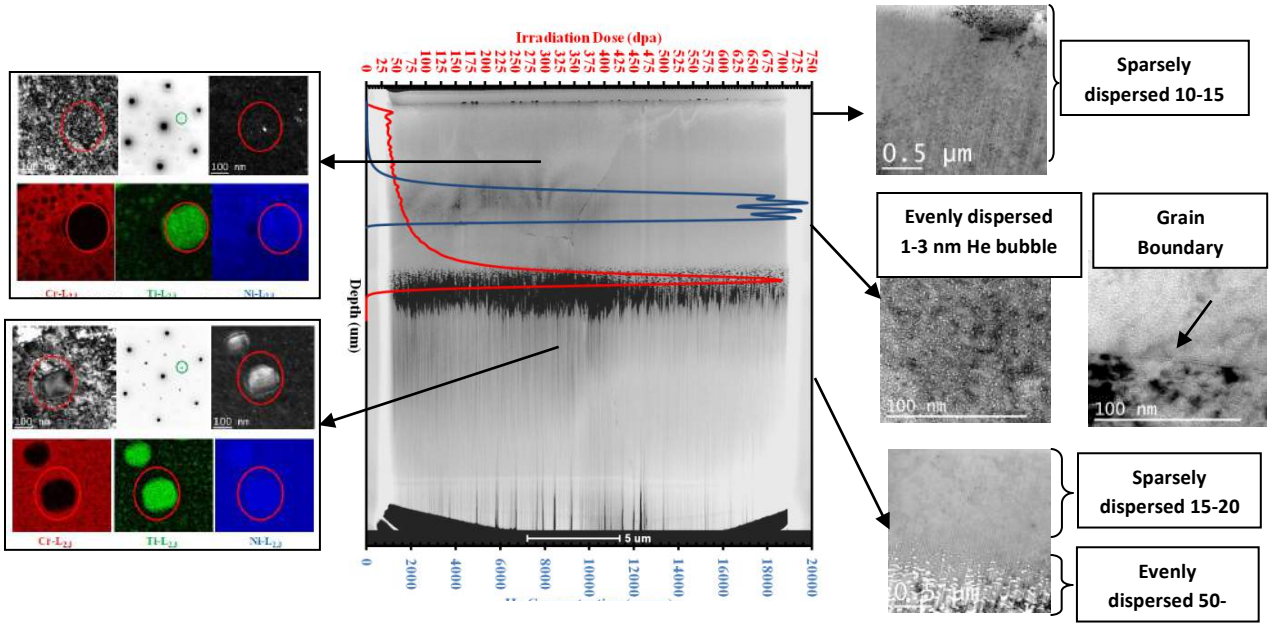

TEM analysis of proton irradiated material (60 dpa, 18000 appm helium). FIB cross section overlaid with irradiation dose and helium profiles (centre); gamma prime characterization including electron diffraction, dark field imaging and EELS spectrum imaging (left); and bright field Fresnel contrast imaging of void and bubble distributions (right).

STUDIES OF DNA IRRADIATION WITH HEAVY IONS

K. Freese[1], D. Gerdes[1], A. Lopez[1], M. Murskyj[1], R. Goldman[2], M. Kang[2], J. Rowley[3], A. Drukier[4]
[1]Department of Physics, University of Michigan
[2]Department of Materials Science and Engineering, University of Michigan
[3]Department of Molecular, Cellular, and Developmental Biology, University of Michigan
[4]BioTraces, Inc.

DNA has many properties that make it an intriguing possibility for next-generation particle detectors capable of reconstructing the trajectories of charged particles to nanometer precision. It can be engineered into precisely specified sequences, can be amplified a billion-fold using readily available techniques, and placed into highly ordered arrays. In concept, a DNA-based particle detector is simple: a "forest" of DNA strands is placed into a rectangular array, some strands are cut by the passage of an energetic charged particle, and the cut-off pieces are collected and sequenced, enabling reconstruction of the trajectory.
A DNA-based particle detector would have diverse applications ranging from mass spectroscopy to novel detectors capable of resolving the direction of astrophysical sources of dark matter. While much is known about DNA irradiation by electrons and protons, irradiation by heavy ions has been far less studied. Our group is investigating this process using the MIBL.

We use a 12410 base-pair plasmid (circular DNA) called pEarleyGate103, which in its natural conformation is in a tightly-wound "supercoiled" state. Cutting one strand causes the plasmid to relax into a circle, while cutting both causes it to linearize. These three topologies can be easily distinguished by their different diffusion rates through an agarose gel. The samples are exposed to a 20 keV Ar beam with fluxes ranging from 10^{10} to 10^{16} ions/cm^2. Preliminary results, from the honors thesis of M. Murskyj, are shown in the middle figure below. The different bands in the gel correspond to zero, one, and two broken strands. By measuring the fraction of single- and double-breaks as a function of radiation dose, we can determine the Ar-DNA cross section. Further work will include improved sample preparation and studies with different energies and beam types.

This work is supported by the University of Michigan MCubed initiative.

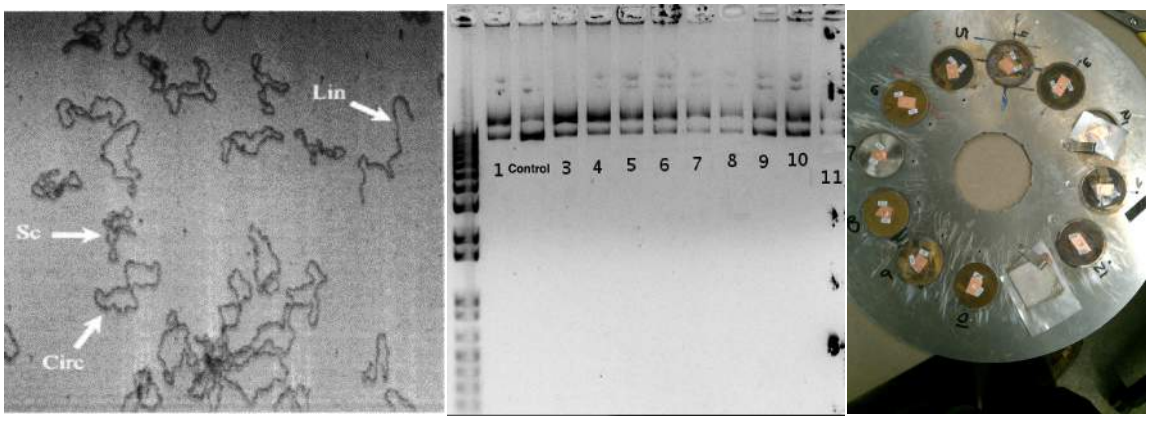

Left: Plasmid DNA in various configurations after irradiation: in its natural supercoiled state (Sc) with two intact strands, in its circularized state after one strand has been nicked (Circ), and in its linearized state after both strands have been broken. Center: Results of running DNA with various radiation exposures through a gel to separate the different geometries. Right: DNA samples on the MIBL target wheel.

CALIBRATION FOR IR MEASUREMENTS OF CARBONATE IN APATITE BY NUCLEAR REACTION ANALYSIS

Y. Zhang[1], K. Clark[1], F. Naab[1]
[1]Department of Earth and Environmental Sciences, University of Michigan
[2]Department of Nuclear Engineering and Radiological Sciences, University of Michigan

Apatite is a widely distributed accessory mineral in igneous rocks. One special aspect of apatite is that it can hold almost all volatile elements in its structure, including H (in the form of OH^-), C (in the form of CO_3^{2-}), S (in the form of SO_4^{2-}), F^-, and Cl^-. Hence, apatite may be used as an indicator of the magmatic volatile environment during apatite formation. To realize this potential, it is necessary to measure the volatile components accurately. This work focuses on the measurement of C in apatite.

Carbonate in apatite can be present in two different sites and several vibrational bands of carbonate in apatite can be detected by infrared (IR) spectroscopy with high sensitivity and precision. However, IR can only provide peak intensities. To convert the intensities to absolute concentrations, it is necessary to calibrate the IR technique against absolute concentrations. We use Nuclear Reaction Analysis (NRA) to determine absolute C concentrations in apatite. The nuclear reaction is $^{12}C(d,p)^{13}C$ (i.e., $^{12}C + {}^2H \rightarrow {}^{13}C + {}^1H$). A high-energy beam of deuteron (^2H) particles bombards the target material (polished apatite crystal). As the particles go into the target, some ^2H particles react with the target nucleus (^{12}C), converting the target nucleus to a new nucleus (^{13}C) and releasing a reaction product (^1H) with a specific amount of energy, which is detected in the NRA proton spectrum at different energy channels. A large channel number means high energy, and small channel number means low energy. The number of counts at each channel number is proportional to the concentration of the target after a matrix correction for the stopping powers. The bombarding particle (^2H) can also react with other nuclei in apatite to produce protons, such as $^{16}O(d,p)^{17}O$, which can be seen in the proton spectrum at lower energy (channel numbers). Because the oxygen concentration in apatite is hundreds to thousands times higher than that of carbon, the oxygen peak is much higher than the carbon peak in an NRA spectrum. The figure shows two NRA spectra of an apatite crystal. The accuracy of the NRA method has been verified by the measurement of a calcite mineral with known carbon concentration.

More work is underway to calibrate the IR method for the analysis of carbonate in apatite using absolute C concentrations from NRA analyses.

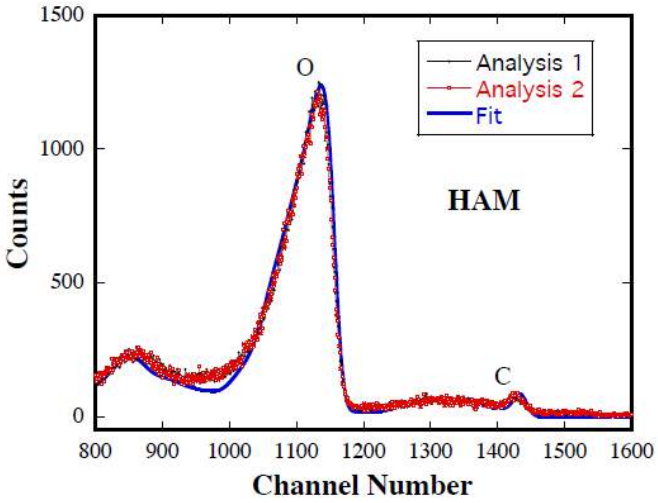

Two NRA spectra showing the analysis of C in an apatite crystal. At channel numbers 1200-1500, there is a peak centered at channel 1426, with a long tail from 1250 to 1400. The peak is due to surface carbon buildup during the analysis, and the long tail is due to reaction of interior carbon with deuteron, reflecting the C concentration in the sample. Repeated analyses of the same spot shows that the surface carbon buildup increases with time almost linearly. The spectra are fit using known apatite composition and basic principles of nuclear reactions, and the fit leads to a C concentration of 900±90 ppm. There are other peaks at lower channel numbers, mostly due to oxygen.

INFLUENCE OF STRAIN LOCALIZATIN ON IASCC OF PROTON-IRRADIATED 304L STAINLSESS STEEL IN SIMULATED PWR PRIMARY WATER

M. Le Millier, J. Crépin, C. Duhamel, A. Pineau, Centre des Matériaux, CNRS UMR 7633, Mines ParisTech, BP 87, F-91003 Evry cedex, France
O. Calonne, L. Fournier, Y. Vidalenc, AREVA NP, France
E. Heripre, Laboratoire de Mécanique des Solides, CNRS UMR 7649, Polytechnique-X-Mines ParisTech, 91128 Palaiseau, France
O. Toader, Michigan Ion Beam laboratory, University of Michigan, USA

304L specimens were irradiated with 2 MeV protons at 360°C to 5 dpa and 10 dpa and strained by CERT in simulated primary water under different loading conditions (monotonic or pseudo-cyclic). In addition to the cracking features study and to correlate crack initiation to crystallographic orientations and strain field measurements, full field analyses were performed by SEM digital imaging correlation technique coupled with EBSD cartography. From 1% of macroscopic deformation, strong heterogeneities appear at a microscopic scale with local values that can reach 8%. The evolution of cracking, correlated with changes in local deformation fields, between 1 and 5% of macroscopic deformation for the pseudo-cyclic test indicates that the cracked boundaries are not necessarily those which present the highest strain after the first step. However, a strong localization was present in their neighborhood. This localization is in the form of narrow lines which can be transgranular or near some grain boundaries. The distribution of normalized deformation shows significant contributions in the "very low" and "very strong" strain ranges associated with a quick spatial alternation. The results obtained for a non-irradiated material is significantly different with high deformation across the grain or group of grains and a distribution more centered on the mean value.

This research is supported by the chair AREVA of Mines ParisTech graduate school.

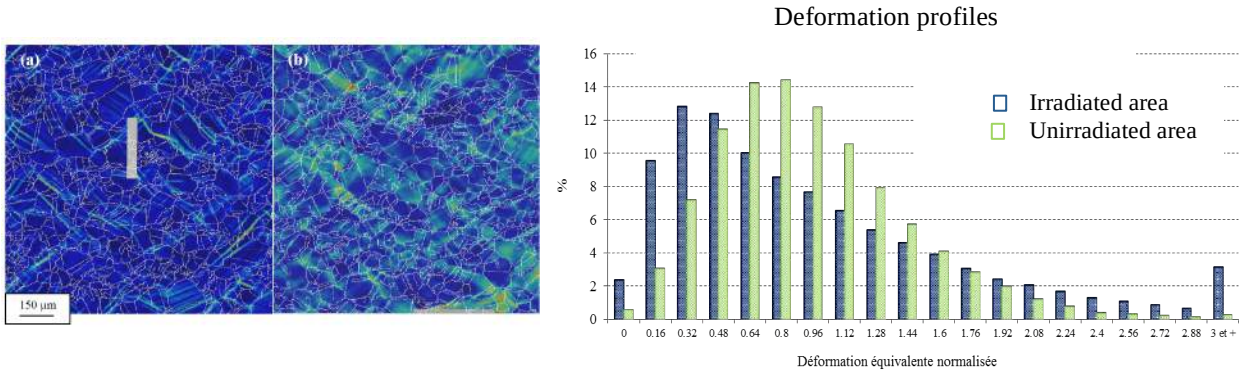

Equivalent Von Mises deformation fields after 1% of macroscopic strain (left) irradiated area (right) non-irradiated area and the deformation distributions.

NANOPARTICLE DYNAMICS IN POLYMER MELTS

C.C. Lin and R.J. Composto
Department of Materials Science and Engineering, University of Pennsylvania

In polymer nanocomposites, particle mobility is critical in that it affects melt flow property, viscosity and composite processability, and it is also crucial in applications such as self-healing materials. The classic Stokes-Einstein (SE) relation describing particle diffusion is no longer valid when particle size is reduced to the length scale of entanglement spacing, and enhanced particle mobility is found in polymer melts both experimentally and theoretically. For example, using the Polymer Reference Interaction Site model (PRISM), Yamamoto and Schweizer[1] found that the diffusion coefficient of the nanoparticle is enhanced by ~10^3 times relative to that predicted by SE relation as the nanoparticle size is half of the entanglement spacing. Using x-ray photon correlation spectroscopy (XPCS), Grabowski et al.[2] investigated the dynamics of gold nanoparticles in poly(*n*-butyl methacrylate) (PBMA) films, and found that gold nanoparticles diffuse ~250 times faster than predicted by SE relation where particle size (radius = 2.5nm) is smaller than the entanglement spacing.

We prepared a diffusion couple composed of a top layer of iron oxide nanoparticles, and a polystyrene layer on the bottom. After the diffusion couple is annealed for appropriate time, the nanoparticles are supposed to diffuse into the polystyrene matrix, and Rutherford backscattering spectrometry (RBS) can be used to probe the depth profile of iron element. Enhanced particle mobility, however, is observed only when particles are individually dispersed while the dynamics follows SE relation when particles aggregate, due to its greater size compared to entanglement spacing. In this set of samples, we found that nanoparticles are immobile using RBS in Michigan Ion Beam Laboratory (MIBL), University of Michigan, due to nanoparticle aggregation confirmed using transmission electron microscope (TEM). Therefore, to measure the diffusion of nanoparticles using this system, we have to make sure that nanoparticles are well-dispersed in polymer matrix. Due to this sample issue, the RBS result obtained in MIBL is different from the result expected.

1. Yamamoto, U.; Schweizer, K. S. *Journal of Chemical Physics* **2011,** 135, (22).
2. Grabowski, C. A.; Adhikary, B.; Mukhopadhyay, A. *Applied Physics Letters* **2009,** 94, (2).

This work is supported by the National Science Foundation NSF/EPSRC Materials World Network DMR-0908449.

HIGH-RESOLUTION SILICON-BASED PARTICLE SENSOR WITH INTEGRATED AMPLIFICATION

S. Svatti
Svaati Scientific LLC, Ann Arbor, MI

The objective of Phase I of this project was to demonstrate that effective multiplication junctions can be composed of thin n+/p+ layers so that the lower energy threshold for high energy particle detection can be extended below few keV range, where the range of ions is particularly small. We successfully made np junction from sub-micrometer thick doped layers, using both short-duration, low temperature annealing, as well as ion implantation. During the project we studied different Avalanche Photo Diode structures on planar silicon radiation detectors. We used the services provided by MIBL, to enable implantation of boron and phosphorous ions at different energy levels and fluences. Post implantation annealing is required in order activate the pn junction, but at the same time our design called for specific spread levels of the ions. Hence we tried different recipes that combined diffusion and implantation processes of ions in different orders of process steps:

1) n+ diffused first /p+ implanted,
2) n+ diffused second/p+ implanted first, and
3) n+ implanted/p+ implanted.

After the successful completion of this project, we hope to continue with Phase II, which will explore other structures such as partitioned electrodes, with guard rings, etc., while refining our design of the APD integrated design of radiation detectors.

INVESTIGATIONS OF IMPURITY EFFECTS IN Cu(In,Ga) Se2 AND CdTe PHOTOVOLTAICS

A. Rocket
Department of Materials Science and Engineering, University of Illinois

MIBL has provided several ion implantations that have supported two different research programs funded by the National Science Foundation and the Department of Energy Office of Energy Efficiency and Renewable Energy (“SunShot”). The implantations have provided us with standards for conducting secondary ion mass spectrometry to determine, for example, the concentration of key impurities in solar cell materials. This is critical to quantitative demonstration of the effects of these impurities on the device performance. The issue is a long-standing problem in the development of these devices.

TEACHING

NERS 425 LABORTORY ON NUCLEAR REACTION ANALYSIS

O. Toader, F. Naab, M. Atzmon
Department of Nuclear Engineering and Radiological Sciences, University of Michigan

For the NERS 425 course, students conducted an experiment to determine the stoichiometry of a Ti_xN_y sample using the reaction between a deuterium particle and a nitrogen nucleus: $N^{14}(d,\alpha)C^{12}$. Nuclear reaction analysis (NRA) is a well-established surface analysis technique. In this method, an energetic particle (deuterium – produced by the Tandem accelerator at MIBL) interacts with the nucleus of an N atom (from the target) to give a reaction product (α particle) that can be measured. The students also use the backscattered yield from an RBS experiment to determine the amount of Ti in the sample by implementing simulation codes like RUMP or SIMNRA with the given experimental spectrum.

This year the experiment was successfully carried out by all the section of the NERS 425 class. During the first meeting of this class, and prior to the experiment, a short tutorial was given to the students on the accelerator, electronics, detectors, software, and vacuum components. After that, they worked independently in a few groups with just the basic support from the MIBL staff (required in the setup of the ion beam and the collection of the spectra). The students decided on a few parameters of the experiment (beam energy, time for spectrum acquisition, etc.) and after that each group obtains spectra similar to the ones in the figure.

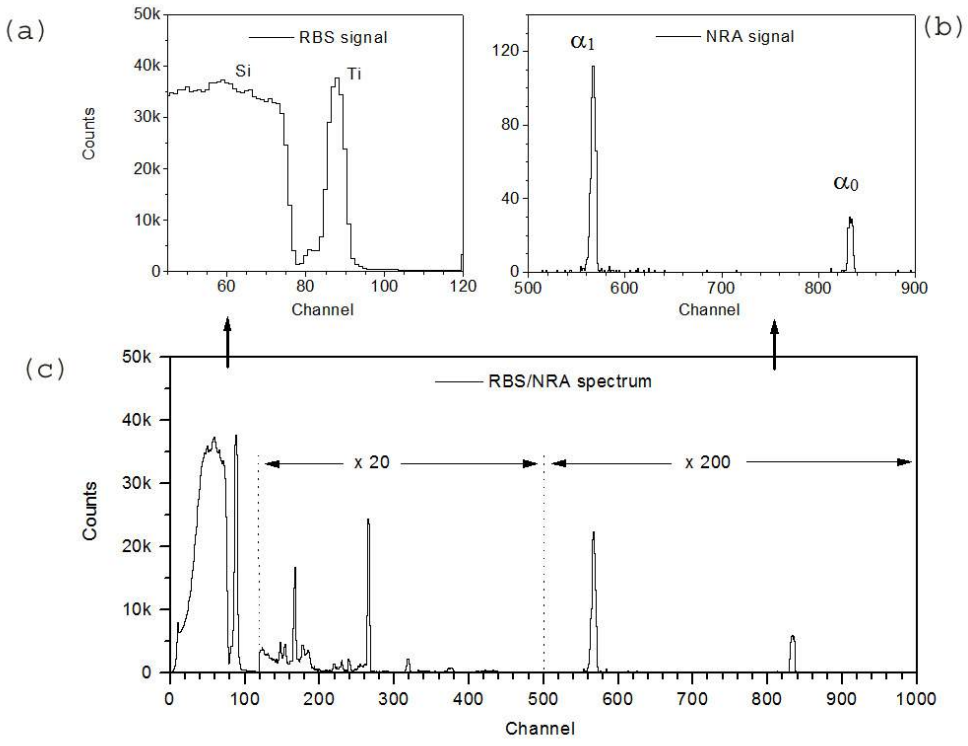

Details of the RBS spectrum (a), the NRA spectrum (b), and typical NRA spectrum for the TiN film obtained during class (c). Conditions: beam energy: 1.4 MeV D^+, solid angle 5 msr., detector angle 150°.

REFERENCES

PUBLICATIONS AND PRESENTATIONS

A. Campbell, G. S. Was, "In situ Proton Irradiation-Induced Creep at Very High Temperature," J. Nucl. Mater. 433 (2013) 86-94.

E. A. Clark, J. Y. Yang, D. Kumar, G. S. Was, C. G. Levi, "Engineered Coatings for Ni Alloys in High Temperature Reactors," Metall. and Mat'ls Trans. A 44A (2013) 835-847.

"Irradiation Assisted Stress Corrosion Cracking," G. S. Was, QNM4, Toronto, CA, June 2013.

"Microstructures of F-M Alloys at Very High Doses," G.S. Was, Symp. Microstructure Processes in Irradiated Materials, TMS Annual Meeting 2013, San Antonio, TX.

"Micromechanics of Dislocation Channeling and IGSCC in Irradiated Stainless Steels," G. S. Was, 19th International Symposium on Plasticity, Nassau, Bahamas, January 2013.

"Role of Helium on Swelling Behavior in Self-Ion Irradiated HT9 Steel," E. Beckett, Z. Jiao, K. Sun, G. Was, Microstructure Processes in Irradiated Materials, TMS Annual Meeting 2013, San Antonio, TX.

"Fission Product Diffusion in β-SiC using Ion-Implanted Multilayer Diffusion Couples," S. Dwaraknath, G. S. Was, Microstructure Processes in Irradiated Materials, TMS Annual Meeting 2013, San Antonio, TX.

"Precipitation in Self-Ion Irradiated Stainless Steels at High Doses," Z. Jiao, E. Beckett, K. Sun, G. S. Was, Microstructure Processes in Irradiated Materials, TMS Annual Meeting 2013, San Antonio, TX.

"Dislocation Loop Contribution to Irradiation creep of F-M Steel T91," C. Xu, G. S. Was, Microstructure Processes in Irradiated Materials, TMS Annual Meeting 2013, San Antonio, TX.

"The Mechanism of Radiation-Induced Segregation in Ferritic-Martensitic Alloys," J. Wharry, G. S. Was, Microstructure Processes in Irradiated Materials, TMS Annual Meeting 2013, San Antonio, TX.

W. He, L. Huang, S. Goddard, E.M. Fozo, P.K. Liaw, "Composition and Surface Tailoring of Zr-based Bulk Metallic Glasses: Implications for Bio-applications", The TMS 143rd Annual Meeting & Exhibition, San Diego, CA, Feb. 15-20, 2014. (Invited talk)

Y. Huang, J.P. Wharry, Z. Jiao, C.M. Parish, S. Ukai, T.R. Allen, "Microstructural evolution in proton irradiated NF616 at 773 K to 3 dpa" J. Nuclear Materials, 442 (2013) 800.

S. M. Bergin, Y.-H. Chen, A.R. Rathmell, P. Charbonneau, Z.-Y. Li, B.J. Wiley, The effect of nanowire length and diameter on the properties of transparent, conducting nanowire films. Nanoscale 2012**,** *4* (6), 1996-2004.

Z. Jiao, G.S. Was, "Precipitates in Self-ion Irradiated Stainless Steels at High Doses" Microstructural Processes in Irradiated Materials Symposium, TMS annual meeting, San Antonio, TX. March 3-7, 2013.

Z. Jiao, Y. Chen, E. Marquis, G.S. Was, "Post-Irradiation Annealing in Mitigation of IASCC of Proton-Irradiated Stainless Steel" 16th International Conference on Environmental Degradation of Materials in Nuclear Power Systems - Water Reactors, Asheville, NC. August 11-15, 2013

Z. Jiao, K, Sun, G.S. Was, “Precipitates Evolution in Ion-Irradiated Ferritic-Martensitic Alloys at High Dose”, 16th International Conference on Fusion Reactor Materials, Beijing, China. October 20-26, 2013

D.D. Osterberg, J. Youngsman, R. Ubic, I.E. Reimanis, D.P. Butt, “Recrystallization kinetics of 3 C silicon carbide implanted with 400 keV Cesium Ions,” J. Am. Ceram. Soc., 96 (2013) 3290-3295.

R. E. Stoller, M. B. Toloczko, G. S. Was, A. G. Certain, S. Dwaraknath, F. Garner, NIM B 310 (2013) 75-80.

L. Tan, T.S. Byun, Y. Katoh, L.L. Snead, G.S. Was, Stability of MX nanoprecipitates in ferritic steels under thermal, stress, and ion irradiation, the 16th International Conference on Fusion Reactor Materials (ICFRM-16), Beijing, China, October 20-26, 2013.

E. A. West, G. S. Was, “Strain Incompatibilities and their Role in Intergranular Cracking of Irradiated 316L Stainless Steel,” J. Nucl. Mater. 441 (2013) 623-632.

C. Xu, G. S. Was, “In-situ Proton Irradiation Creep of Ferritic-Martensitic Steel T91,” J. Nucl. Mater. 441 (2013) 687-687.

S. J. Zinkle and G. S. Was, “Materials Challenges in Nuclear Energy,” Acta Mater. Diamond Jubilee Issue, 61 (2013) 735-758.